令和２年度卒業論文

揺らぐ拡散係数を導入したダンベルモデルのダイナミクス

物理工学科

増渕研究室

学生番号： 081720143

氏名： 北村仁哉

Abstract

The Hookean dumbbell model, which describes a polymer as two Brownian beads connected by the Hookean spring, is the most simple model for polymer dynamics. In this model, the center of mass exhibits normal diffusion, and the relaxation has a single exponential decay. However, in some dynamic heterogeneous systems such as glassy polymers and entangled polymers, anomalous diffusion is observed. For a single particle, there are some models to describe the anomalous diffusion. The fluctuating diffusivity (FD) model is a model that regards diffusivity as a time-dependent fluctuating variable. The FD models describe the non-Gaussianity for the displacement distribution. In this work, we introduce the FD model to the dumbbell model. We assume that the spatial scale of the heterogeneity is comparable to the size of the polymer. With this assumption, the diffusivities of each bead could be different from each other. Hence we introduce the independent FD to each bead. We calculate the mean squared displacement (MSD) of the center of mass, the end-to-end relaxation, and the relaxation modulus analytically, with the transfer operator method. As a result, we find that the center of mass exhibits a sub-diffusion, and the end-to-end relaxation and the relaxation modulus exhibit multi-mode exponential decay. Besides, we reproduce the results of molecular simulations for supercooled polymer, and the fitting parameters are corresponding to a physical picture of the supercooled liquids.

Contents

Chapter 1

Introduction

Some physical properties of polymers such as diffusion and viscoelasticity outcome from the molecular dynamics of the polymers. To describe or predict the properties, a lot of coarse-grained models for polymers have been developed[1, 2, 3].

The Hookean dumbbell model [1] (hereinafter the dumbbell model) is the simplest model to describe the molecular dynamics of polymers. The dumbbell consists of two Brownian particles connected by a linear spring. Each Brownian particle represents a group of monomers that compose a polymer chain. The elastic force due to the linear spring represents the entropic elasticity. Owning to the construction, we can calculate various properties analytically. For instance, the center of mass (c.m.) exhibits a normal diffusion, i.e., the mean squared displacement (MSD) is entirely proportional to time. The end-to-end relaxation of the bond vector and the relaxation modulus exhibits a single exponential decay.

Mainly toward the rheological modeling of polymeric fluids, there have been a lot of extensions for the dumbbell model. The modification of the dumbbell model can be classified into i) the modification of the spring and ii) the modification of the mobility tensor of the Brownian beads. In the FENE dumbbell model [4], a finitely extensible non-linear elastic (FENE) spring is introduced instead of the linear spring to represent the fact that a polymer chain cannot be extended to an infinite length. the FENE dumbbell was introduced for the extensional behavior of polymers[4], and it was applied for the shear rheology as well[4, 5]. As the other approach, the mobility tensor was replaced by the Oseen tensor for the hydrodynamic interaction [6], and by the anisotropic mobility tensor for the entanglement effect [7]. These extensions reasonably predict some non-linear rheological responses of polymers.

Nevertheless, we note that most of the dumbbell models exhibit the normal diffusion for the c.m. This is rational because the internal force acting on the Brownian beads does not affect the motion of the c.m. In this respect, the dumbbell models do not represent the sub-diffusive motion of polymeric systems such as glassy and entangled systems.

Meanwhile, the sub-diffusion has been analyzed by the single-particle models. One of such models is the continuous-time random walks (CTRW) [8], which is the theory describing the hopping motion of a particle in a disordered lattice. In the CTRW, the particle is trapped for a waiting time until the particle hops to the next lattice site. The jump size and the waiting time are sampled from the distribution, and the sub-diffusion is obtained given that the waiting time distribution realizes a finite mean-waiting time. With such a condition, the system does not reach equilibrium and the CTRW is used to describe the weak ergodicity breaking in spin glasses [9]. Also, the CTRW assumption is natural for biological systems in terms of the chemical attachments which have a broad distribution for the reaction times [10], and the CTRW is applied

for many biological systems [11, 12]. Another approach is the generalized Langevin equation (GLE) [13, 14] which has a memory effect in friction term of the Langevin equation. The GLE is derived by the projection operator applied to the Hamilton equation, and the GLE is exact when the Gaussian assumption for the fast variables is justified. The GLE can describe the sub-diffusion of the single-particle with a particular memory kernel [13], and the memory kernel is uniquely determined from the MSD [13]. We can obtain the viscoelasticity of the system from the MSD data of the single-particle by the generalized Einstein-Stokes relation [15].

Though the CTRW and the GLE are broadly applied for many systems, the applicability is still controversial. In particular, CTRW cannot describe the sub-diffusion with the equilibrium waiting time distribution. (it is cannot be used for equilibrium systems.) Besides, since the CTRW does not include external forces explicitly, we cannot use the CTRW for the systems under external forces. Concerning the GLE, due to the Gaussian assumption of the fast variables, it cannot describe the non-Gaussianity of the probability density function (PDF) of the displacement, which is for example observed in supercooled liquids [16] and biological systems [17, 18].

Toward these problems, the fluctuating diffusivity (FD) models have been developed in recent years. In the FD models, the diffusivity is regarded as a time-dependent random fluctuating value. They are studied recently in many contexts, in which the non-Gaussianity of PDF of displacement of the single-particle is observed in dynamic heterogeneous environments [19, 20, 21]. These models describe the spatial and temporal dynamic heterogeneity by embedding it into the time-dependent fluctuation of the diffusivity. Since the FD models are described by the Langevin equation, they can include external forces on the particle [22], and there is no restriction on whether the system is non-equilibrium or not. There are some typical models of FDs. One of them is the Two-state (TS) model [19], in which the diffusivity is assumed to flip between only two values. These two values represent the approximated mobility in such supercooled liquids [23]. The other is the diffusing diffusivity (DD) model [24, 20]. The DD model is a continuous FD model, where the diffusivity is the squared value of a vector that obeys an Ornstein–Uhlenbeck process. The DD model describes the Brownian-yet-non-Gaussian diffusion, which means though the particle exhibits the normal diffusion, the PDF is not Gaussian distribution. Besides, the fluctuation behavior of the diffusivity is observed in entangled polymer melt [25] by calculating the MSD with finite time (called time-averaged MSD (TAMSD) in [25]).

Two earlier studies use the FD for the dynamics of polymers. One of them introduces the general FD to the dumbbell model [22]. In this model, the diffusivities are the same in the two Brownian beads. This model results in that the c.m. exhibits normal diffusion, and the end-to-end relaxation of the bond vector has multiple correlation modes. The other one introduces the DD model to the Langevin equation of each mode in the Rouse model [26]. Although the target polymer model is different from that of [22], the Langevin equations in each model are almost the same and the result of [26] is similar to the result of [22].

However, especially in dynamic heterogeneous environments, the diffusivity may be different for each position. Therefore, the assumption that each Brownian bead located at a different position has the same diffusivity may not be correct when the dynamic heterogeneity is observed in the smaller range than the size of polymers. In other words, the diffusivities could be different in each Brownian bead to describe the dynamics of polymers in dynamic heterogeneous environments.

In this work, we propose a new model for polymers in the dynamic heterogeneous environment such as glassy polymer melts by introducing the FD to the Hookean dumbbell model. In this model, the diffusivities of the Brownian beads are not common in the dumbbell. Hereinafter,

we call this model as the FD dumbbell model. We calculate the MSD of the c.m., the end-to-end relaxation of the bond vector, and the relaxation modulus analytically, and compare them with those of the Hookean dumbbell model. Afterwards, we attempt to describe the dynamics of an unentangled glassy polymer melt and an entangled polymer melt by using the FD dumbbell model.

Chapter 2

Model

2.1 Hookean dumbbell model

Let us consider a dumbbell that consists of two Brownian beads connected by a Hookean spring. The dynamics of each Brownian bead of the dumbbell in a n spatial dimension space is described by the Langevin equations that do not have the ballistic term as shown below.

$$\begin{cases} \mathbf{0} = -\dfrac{nk_BT}{\bar{Q}^2}(\boldsymbol{R}_1 - \boldsymbol{R}_2) - \gamma\dfrac{d\boldsymbol{R}_1}{dt} + \sqrt{2\gamma k_BT}\boldsymbol{w}_1(t), & \text{(2.1a)} \\ \mathbf{0} = -\dfrac{nk_BT}{\bar{Q}^2}(\boldsymbol{R}_2 - \boldsymbol{R}_1) - \gamma\dfrac{d\boldsymbol{R}_2}{dt} + \sqrt{2\gamma k_BT}\boldsymbol{w}_2(t), & \text{(2.1b)} \end{cases}$$

where $\boldsymbol{R}_j$ is the position of j th Brownian bead, γ is a friction coefficient, k_B is the Boltzmann constant, and T is the temperature. $\boldsymbol{w}_j(t)$ is the Gaussian white noise, which obeys

$$\langle \boldsymbol{w}_j(t) \rangle = \mathbf{0}, \tag{2.2}$$

$$\left\langle \boldsymbol{w}_j(t)\boldsymbol{w}_k(t') \right\rangle = \delta_{jk}\delta(t-t')\mathbf{1}, \tag{2.3}$$

where $j, k = 1, 2$, $\mathbf{0}$ is the zero vector, and $\mathbf{1}$ is the unit tensor. The first term in the right-hand side of Eqs. (2.1) represents the elastic forces and the coefficients $nk_BT/\bar{Q}^2$ are calculated by the theory of entropic elasticity. $\bar{Q}$ is called the segment size, and the squared value is equal to the statistical average of $|\boldsymbol{R}_1 - \boldsymbol{R}_2|^2$. The second term in the right-hand side of Eqs. (2.1) represents the friction force, and the third term is the thermal fluctuation force. They are caused by the many collisions of surrounding fluid particles. We can justify the Gaussian nature of the fluctuation forces by the central limit theorem for the infinitesimal time average of the impulsive forces caused by the collisions. The coefficient $\sqrt{2\gamma k_BT}$ is from the fluctuation-dissipation relation, which keeps the balance between the dissipation by the friction force and the fluctuation force in the equilibrium state. We introduce the diffusivity D by using the Einstein-Stokes relation

$$D = \frac{k_BT}{\gamma}, \tag{2.4}$$

and rewrite Eq. (2.1) as

$$\begin{cases} \dfrac{d\boldsymbol{R}_1}{dt} = -\dfrac{nD}{\bar{Q}^2}(\boldsymbol{R}_1 - \boldsymbol{R}_2) + \sqrt{2D}\boldsymbol{w}_1(t), & \text{(2.5a)} \\ \dfrac{d\boldsymbol{R}_2}{dt} = -\dfrac{nD}{\bar{Q}^2}(\boldsymbol{R}_2 - \boldsymbol{R}_1) + \sqrt{2D}\boldsymbol{w}_2(t). & \text{(2.5b)} \end{cases}$$

The c.m. of the dumbbell defined as $\boldsymbol{X}_0 := (\boldsymbol{R}_1 + \boldsymbol{R}_2)/2$ and the bond vector defined as $\boldsymbol{X}_1 := \boldsymbol{R}_1 - \boldsymbol{R}_2$ obey the following Langevin equation.

$$\begin{cases} \dfrac{d\boldsymbol{X}_0}{dt} = \dfrac{\sqrt{2D}\boldsymbol{w}_1(t) + \sqrt{2D}\boldsymbol{w}_2(t)}{2}, & \text{(2.6a)} \\ \dfrac{d\boldsymbol{X}_1}{dt} = -2\alpha D\boldsymbol{X}_1 + \sqrt{2D}\boldsymbol{w}_1(t) - \sqrt{2D}\boldsymbol{w}_2(t), & \text{(2.6b)} \end{cases}$$

where $\alpha := n/\bar{Q}^2$. From Eq. (2.6a), we can calculate the MSD of the c.m. as

$$\left\langle [\boldsymbol{X}_0(t) - \boldsymbol{X}_0(0)]^2 \right\rangle = nDt. \tag{2.7}$$

The meaning of Eq. (2.7) is that the polymer represented by the dumbbell exhibits the normal diffusion entirely. From Eq. (2.6b), the end-to-end relaxation can be calculated as

$$\langle \boldsymbol{X}_1(t) \cdot \boldsymbol{X}_1(0) \rangle = \frac{n}{\alpha} \exp\left(-2\alpha Dt\right). \tag{2.8}$$

The end-to-end relaxation is related to the rotational relaxation of the dumbbell. Also, in the $n = 2, 3$ dimension space which has a coordinates of (x, y) or (x, y, z), the stress at the time t is calculated as the Kramers form :

$$\begin{aligned} \hat{\boldsymbol{\sigma}}(\boldsymbol{X}_1) &= \frac{1}{V}\frac{\partial \mathcal{F}(\boldsymbol{X}_1)}{\partial \boldsymbol{X}_1} \\ &= \frac{\alpha k_B T}{V}\boldsymbol{X}_1\boldsymbol{X}_1, \end{aligned} \tag{2.9}$$

where the $\mathcal{F}$ is the free energy by the entropic elasticity defined as $\mathcal{F}(\boldsymbol{X}_1) := \alpha k_B T(\boldsymbol{X}_1 \cdot \boldsymbol{X}_1)/2$, and V represents the volume of the system. The shear relaxation modulus for one polymer can be calculated by the Green-Kubo formula [27] :

$$G(t) = \frac{V}{k_B T}\left\langle \hat{\sigma}_{xy}(t)\hat{\sigma}_{xy}(0) \right\rangle = \frac{k_B T}{V}\alpha^2 \left\langle [X_{1x}(t)X_{1y}(t)][X_{1x}(0)X_{1y}(0)] \right\rangle \tag{2.10}$$

$$= \frac{k_B T}{V}\exp(-4\alpha Dt), \tag{2.11}$$

where $\hat{\sigma}_{xy}$ is the xy component of the stress tensor Eq. (2.9) and $\boldsymbol{X}_{1h}$ for $h = x, y$ is the h component of $\boldsymbol{X}_1$. From Eqs. (2.8) and (2.11), the end-to-end relaxation and the relaxation modulus exhibits the single exponential decay.

2.2 FD dumbbell model

Now, let us modify the dumbbell model shown above by introducing the FD to two beads. The Langevin equations for the beads are written as follows.

$$\begin{cases} \dfrac{d\boldsymbol{R}_1}{dt} = -\dfrac{n}{\bar{Q}^2}D_1(t)(\boldsymbol{R}_1 - \boldsymbol{R_2}) + \sqrt{2D_1(t)}\boldsymbol{w}_1(t), & \text{(2.12a)} \\ \dfrac{d\boldsymbol{R}_2}{dt} = -\dfrac{n}{\bar{Q}^2}D_2(t)(\boldsymbol{R}_2 - \boldsymbol{R_1}) + \sqrt{2D_2(t)}\boldsymbol{w}_2(t). & \text{(2.12b)} \end{cases}$$

$D_j(t)$ is the diffusivity for j th Brownian bead. Note that the diffusivity of one Brownian bead is not always equal to the other, though the diffusivities can correlate with each other. Let us rewrite Eqs. (2.12) according to the c.m. $\boldsymbol{X}_0$ and the bond vector $\boldsymbol{X}_1$ as shown below.

$$\begin{cases} \dfrac{d\boldsymbol{X}_0}{dt} = -\dfrac{\alpha}{2}\Delta D(t)\boldsymbol{X}_1 + \bar{\boldsymbol{\Xi}}(t), & \text{(2.13a)} \\ \dfrac{d\boldsymbol{X}_1}{dt} = -2\alpha\bar{D}(t)\boldsymbol{X}_1 + \Delta\boldsymbol{\Xi}(t). & \text{(2.13b)} \end{cases}$$

Here, we have these values :

$$\bar{D}(t) := \frac{D_1(t) + D_2(t)}{2}, \tag{2.14}$$

$$\Delta D(t) := D_1(t) - D_2(t), \tag{2.15}$$

$$\bar{\boldsymbol{\Xi}}(t) := \frac{\sqrt{2D_1(t)}\boldsymbol{w}_1(t) + \sqrt{2D_2(t)}\boldsymbol{w}_2(t)}{2}, \tag{2.16}$$

$$\Delta\boldsymbol{\Xi}(t) := \sqrt{2D_1(t)}\boldsymbol{w}_1(t) - \sqrt{2D_2(t)}\boldsymbol{w}_2(t). \tag{2.17}$$

The statistical averages of $\bar{\boldsymbol{\Xi}}(t)$ and $\Delta\boldsymbol{\Xi}(t)$ and over $\boldsymbol{w}_j(t)$ are written as

$$\left\langle \bar{\boldsymbol{\Xi}}(t) \right\rangle_{\boldsymbol{w}} = \boldsymbol{0}, \tag{2.18}$$

$$\left\langle \Delta\boldsymbol{\Xi}(t) \right\rangle_{\boldsymbol{w}} = \boldsymbol{0}. \tag{2.19}$$

The correlations among $\bar{\boldsymbol{\Xi}}(t)$ and $\Delta\boldsymbol{\Xi}(t)$ averaged over $\boldsymbol{w}_j(t)$ are written as

$$\left\langle \bar{\boldsymbol{\Xi}}(t)\bar{\boldsymbol{\Xi}}(t') \right\rangle_{\boldsymbol{w}} = \bar{D}(t)\delta(t-t')\boldsymbol{1}, \tag{2.20}$$

$$\left\langle \Delta\boldsymbol{\Xi}(t)\Delta\boldsymbol{\Xi}(t') \right\rangle_{\boldsymbol{w}} = 4\bar{D}(t)\delta(t-t')\boldsymbol{1}, \tag{2.21}$$

$$\left\langle \bar{\boldsymbol{\Xi}}(t)\Delta\boldsymbol{\Xi}(t') \right\rangle_{\boldsymbol{w}} = \Delta D(t)\delta(t-t')\boldsymbol{1}. \tag{2.22}$$

In comparison between Eqs (2.6a) and (2.13a), the FD dumbbell has an extra term that expresses the coupling between the motion of the c.m. and the fluctuation of the bond vector. The extra term outcomes from that the diffusivity of one Brownian bead is not always equal to the other. This term has an important effect on the diffusion of the c.m. as shown in the next section.

Chapter 3

Theory

In this section, we calculate the analytical solutions of the statistical values for the FD dumbbell model. We use the transfer operator method, which is introduced by Uneyama et al. for the analysis of the Ornstein-Uhlenbeck process with the FD (OUFD) [22]. Owning to their calculation, we obtain the analytical solutions for a general FD model. Afterwards, we introduce the TS model instead of the general FD model as an example.

3.1 Calculation of analytical solutions by transfer operator method

In the first place, let us start from the calculation of the MSD of the c.m. of the FD dumbbell model. Since Eq. (2.13a) includes the fluctuation of the bond vector, we have to calculate the solution for Eq. (2.13b) not only the solution for Eq. (2.13a). The solution of Eq. (2.13a) is

$$\boldsymbol{X}_0(t) = \boldsymbol{X}_0(0) + \int_0^t d\tau \bar{\boldsymbol{\Xi}}(\tau) - \frac{\alpha}{2}\int_0^t d\tau \Delta D(\tau)\boldsymbol{X}_1(\tau), \tag{3.1}$$

and the solution of Eq. (2.13b) can be given by

$$\boldsymbol{X}_1(t) = \exp\left[-2\alpha\int_0^t d\tau \bar{D}(\tau)\right]\boldsymbol{X}_1(0) + \int_0^t d\tau \exp\left[-2\alpha\int_\tau^t d\tau' \bar{D}(\tau')\right]\Delta\boldsymbol{\Xi}(\tau). \tag{3.2}$$

From Eq. (3.1), the MSD of the c.m. is calculated as

$$\begin{aligned}\left\langle [\boldsymbol{X}_0(t) - \boldsymbol{X}_0(0)]^2 \right\rangle =& n\left\langle \bar{D}\right\rangle t \\ &- \alpha\int_0^t d\tau \int_0^t d\tau' \left\langle \Delta D(\tau)\boldsymbol{X}_1(\tau)\cdot\bar{\boldsymbol{\Xi}}(\tau')\right\rangle \\ &+ \frac{\alpha^2}{4}\int_0^t d\tau \int_0^t d\tau' \left\langle \Delta D(\tau)\Delta D(\tau')\boldsymbol{X}_1(\tau)\cdot\boldsymbol{X}_1(\tau')\right\rangle.\end{aligned} \tag{3.3}$$

By substituting Eq. (3.2) to Eq. (3.3), we obtain the MSD of the c.m. as shown below. The detailed calculation is shown in Appendix A.

$$
\begin{aligned}
&\left\langle [\boldsymbol{X}_0(t) - \boldsymbol{X}_0(0)]^2 \right\rangle - n \left\langle \bar{D} \right\rangle t \\
=& -n\alpha \int_0^t d\tau \int_0^\tau d\tau' \left\langle \Delta D(\tau) \exp\left[-2\alpha \int_{\tau'}^\tau d\upsilon \bar{D}(\upsilon) \right] \Delta D(\tau') \right\rangle \\
&+ \frac{n\alpha}{2} \int_0^t d\tau \int_0^\tau d\tau' \left\langle \Delta D(\tau)\Delta D(\tau') \exp\left[-2\alpha \int_0^\tau d\upsilon \bar{D}(\upsilon) - 2\alpha \int_0^{\tau'} d\upsilon' \bar{D}(\upsilon') \right] \right\rangle \\
&+ 2n\alpha^2 \int_0^t d\tau \int_0^\tau d\tau' \int_0^{\tau'} d\tau'' \left\langle \Delta D(\tau)\Delta D(\tau') \exp\left[-2\alpha \int_{\tau''}^\tau d\upsilon \bar{D}(\upsilon) - 2\alpha \int_{\tau''}^{\tau'} d\upsilon' \bar{D}(\upsilon') \right] \bar{D}(\tau'') \right\rangle .
\end{aligned}
\tag{3.4}
$$

Hereafter, we represent the integrands in Eq. (3.4) as the correlation functions defined as follows.

$$
\Phi(t,t') = \left\langle \Delta D(t) \exp\left[-2\alpha \int_{t'}^t d\tau \bar{D}(\tau) \right] \Delta D(t') \right\rangle . \tag{3.5}
$$

$$
\Psi(t,t') = \left\langle \Delta D(t)\Delta D(t') \exp\left[-2\alpha \int_0^t d\tau \bar{D}(\tau) - 2\alpha \int_0^{t'} d\tau' \bar{D}(\tau') \right] \right\rangle . \tag{3.6}
$$

$$
\Omega(t,t',t'') = \left\langle \Delta D(t)\Delta D(t') \exp\left[-2\alpha \int_{t''}^t d\tau \bar{D}(\tau) - 2\alpha \int_{t''}^{t'} d\tau' \bar{D}(\tau') \right] \bar{D}(t'') \right\rangle . \tag{3.7}
$$

Below, we shall calculate $\Phi(t)$, $\Psi(t,t')$ and $\Omega(t,t',t'')$ and integrate it to calculate MSD of the c.m. analytically.

To obtain the analytical solution of Eq. (3.4), we calculate the correlation functions Eqs.(3.5)-(3.7) by using the transfer operator method. To calculate Eq. (3.19), we introduce a path probability $\mathcal{P}[\xi]$, which is the probability of a certain path $\xi(t)$, and rewrite $D(t)$ as a function of path $\xi(t)$ like $D(t) = D(\xi(t))$.

$$
\Phi(t,t') = \int \mathcal{D}\xi \ \Delta D(\xi(t)) \exp\left[-2\alpha \int_{t'}^t d\tau \bar{D}(\xi(\tau)) \right] \Delta D(\xi(t'))\mathcal{P}[\xi]. \tag{3.8}
$$

We introduce a discrete time $\tau \approx \tau_i = i\ \delta\tau$, then $\xi(\tau)$ and $\Delta D(\tau)$ can be rewritten as

$$
\xi(\tau) \approx \xi(\tau_i) = \xi_i, \tag{3.9}
$$

$$
\Delta D(\tau) = \Delta D(\xi(\tau)) \approx \Delta D(\xi_i). \tag{3.10}
$$

Further, we rewrite $\mathcal{P}[\xi]$ as $\mathcal{P}[\xi] = \exp(-\mathcal{S}[\xi])$. If $\xi(t)$ is a Markovian stochastic process, we can rewrite $\mathcal{S}[\xi]$ as

$$
\mathcal{S}[\xi] \approx \delta\tau \sum_i s(\xi_{i+1}, \xi_i). \tag{3.11}
$$

Then, we can rewrite Eq. (3.8) as follows :

$$\begin{aligned}\Phi(t,t') &\approx \int \prod_{i=t'/\delta\tau}^{t/\delta\tau} d\xi_i \Delta D(\xi(t)) \exp\left[-2\alpha\delta\tau \sum_{i=t'/\delta\tau}^{t/\delta\tau-1} \Delta D(\xi_i)\right] \exp\left[\delta\tau \sum_{i=t'/\delta\tau}^{t/\delta\tau-1} s(\xi_{i+1},\xi_i)\right] \Delta D(\xi_{t'/\delta\tau}) P(\xi_{t'/\delta\tau}) \\ &= \int \prod_{i=t'/\delta\tau}^{t/\delta\tau} d\xi_i \Delta D(\xi(t)) \exp\left[-\delta\tau \sum_{i=t'/\delta\tau}^{t/\delta\tau-1} \left\{s(\xi_{i+1},\xi_i) + 2\alpha\bar{D}(\xi_i)\right\}\right] \Delta D(\xi_{t'/\delta\tau}) P(\xi_{t'/\delta\tau}).\end{aligned} \tag{3.12}$$

Here, we performed the functional integral over $\xi(\tau)$ for $\tau < t'$ and $t < \tau$. Since the correlation function is only dependent on $\xi(\tau)$ with $t' < \tau < t$, the functional integral over $\xi(\tau)$ for $\tau < t'$ is the probability distribution function $P(\xi_{t'/\delta t})$ and the functional integral over $\xi(\tau)$ for $t < \tau$ is unity. Since we discuss in an equilibrium state, we define $P(\xi_{t'/\delta t})$ as the equilibrium probability distribution as $P(\xi_{t'/\delta t}) = P_{\rm eq}(\xi_{t'/\delta t})$.

The factor $e^{-\delta\tau s(\xi_{i+1},\xi_i)}$ represents the probability of transition from ξ_i to ξ_{i+1}. Thus,

$$P(\xi_{i+1}, t_{i+1}) = \int d\xi_i e^{-\delta\tau s(\xi_{i+1},\xi_i)} P(\xi_i, t_i), \tag{3.13}$$

where $P(\xi, t)$ is an arbitrary function.

Meanwhile, the probability distribution of ξ at a certain time t follows a master equation

$$\frac{\partial P(\xi,t)}{dt} = \hat{\mathcal{L}} P(\xi,t), \tag{3.14}$$

where $P(\xi, t)$ is the probability distribution function. Eq. (3.14) can be solved as

$$P(\xi, t_{i+1}) = e^{\delta\tau\hat{\mathcal{L}}} P(\xi, t_i). \tag{3.15}$$

By comparing Eq. (3.13) and Eq. (3.15), for any arbitral functions, we obtain

$$\int d\xi_i e^{-\delta\tau s(\xi_{i+1},\xi_i)} P(\xi_i) = e^{\delta\tau\hat{\mathcal{L}}} P(\xi_{i+1}). \tag{3.16}$$

We introduce a transfer operator $\hat{\mathcal{W}}$ as

$$\begin{aligned} e^{-\delta\tau\hat{\mathcal{W}}} P(\xi_{i+1}) &= \int d\xi_i \exp\left[-\delta\tau\left\{s(\xi_{i+1},\xi_i) + 2\alpha\bar{D}(\xi_i)\right\}\right] P(\xi_i) \\ &= e^{\delta\tau\hat{\mathcal{L}}}\left[e^{-2\delta\tau\alpha\bar{D}(\xi_{i+1})} P(\xi_{i+1})\right]. \end{aligned} \tag{3.17}$$

By expanding Eq. (3.17) keeping only the leading-order term, we can express $\hat{\mathcal{W}}$ as

$$-\hat{\mathcal{W}} P(\xi) \approx \left[\hat{\mathcal{L}} - 2\alpha\bar{D}(\xi)\right] P(\xi). \tag{3.18}$$

At the limit of $\delta\tau \to 0$, Eq. (3.18) is exact. From Eq. (3.17), we can calculate Eq. (3.12) as

$$\Phi(t,t') = \int d\xi\ \Delta D(\xi) e^{-(t-t')\hat{\mathcal{W}}} \Delta D(\xi) P_{\rm eq}(\xi). \tag{3.19}$$

In a similar way, we can calculate Eq. (3.6) and Eq. (3.7) as shown below. The detailed calculation is shown in Appendix B

$$\Psi(t,t') = \int d\xi \Delta D(\xi) e^{-(t-t')\hat{\mathcal{W}}} \Delta D(\xi) e^{-t'\hat{\mathcal{V}}} P(\xi). \tag{3.20}$$

$$\Omega(t,t',t'') = \int d\xi \Delta D(\xi) e^{-(t-t')\hat{\mathcal{W}}} \Delta D(\xi) e^{-(t'-t'')\hat{\mathcal{V}}} \bar{D}(\xi) P(\xi). \tag{3.21}$$

Here, $\hat{\mathcal{V}}$ is the transfer operator which is defined as shown below.

$$\begin{aligned} e^{-\delta\tau\hat{\mathcal{V}}} P(\xi_{i+1}) &= \int d\xi_i \exp\left[-\delta\tau\left\{s(\xi_{i+1},\xi_i) + 4\alpha\bar{D}(\xi_i)\right\}\right] P(\xi_i) \\ &= e^{\delta\tau\hat{\mathcal{L}}}\left[e^{-4\delta\tau\alpha\bar{D}(\xi_{i+1})} P(\xi_{i+1})\right]. \end{aligned} \tag{3.22}$$

We use change of variables :

$$\begin{cases} t' = \tau - \tau', & \text{(3.23a)} \\ s' = \tau', & \text{(3.23b)} \end{cases}$$

for the integral in the second line and the third line of Eq. (3.4), and

$$\begin{cases} t' = \tau - \tau', & \text{(3.24a)} \\ s' = \tau' - \tau'', & \text{(3.24b)} \\ u' = \tau'', & \text{(3.24c)} \end{cases}$$

for the integral in the fourth line of Eq. (3.4), and Eq. (3.4) can be calculated analytically as shown below.

$$\begin{aligned} \left\langle [\boldsymbol{X}_0(t) - \boldsymbol{X}_0(0)]^2 \right\rangle =& n\left\langle \bar{D} \right\rangle t - n\alpha \int_0^t dt'(t-t')\Phi(t') \\ &+ \frac{n\alpha}{2} \int_0^t dt' \int_0^{t-t'} ds' \Psi(t',s') + 2n\alpha^2 \int_0^t dt' \int_0^{t-t'} ds'(t-t'-s')\Omega(t',s'), \end{aligned} \tag{3.25}$$

where

$$\Phi(t) = \int d\xi\ \Delta D(\xi) e^{-t\hat{\mathcal{W}}} \Delta D(\xi) P_{\mathrm{eq}}(\xi), \tag{3.26}$$

$$\Psi(t,s) = \int d\xi \Delta D(\xi) e^{-t\hat{\mathcal{W}}} \Delta D(\xi) e^{-s\hat{\mathcal{V}}} P_{\mathrm{eq}}(\xi), \tag{3.27}$$

$$\Omega(t,s) = \int d\xi \Delta D(\xi) e^{-t\hat{\mathcal{W}}} \Delta D(\xi) e^{-s\hat{\mathcal{V}}} \bar{D}(\xi) P_{\mathrm{eq}}(\xi). \tag{3.28}$$

The detailed integral calculation is shown in Appendix C.

Eq. (3.25) shows that the c.m. may exhibit an anomalous diffusion if the contributions of the other terms rather than the first term are not negligible. Besides, by considering the order of the integral, The c.m. shows a sub-diffusion at the diffusion time close to the relaxation times of $\Phi(t)$, $\Psi(t,s)$, and $\Omega(t,s)$. Note that all of the relaxation functions $\Phi(t)$, $\Psi(t,s)$, and $\Omega(t,s)$ have the ΔD term. This means the sub-diffusion results from the coupling term in Eq. (2.13a).

At the limit of $t \to 0$, the double integrals over t' and s' in Eq. (3.25) give $\mathcal{O}(t^2)$ and $\mathcal{O}(t^3)$ terms. By neglecting these terms, we have the following expression.

$$\left\langle [\boldsymbol{X}_0(t) - \boldsymbol{X}_0(0)]^2 \right\rangle \to n \left\langle \bar{D} \right\rangle t. \ (t \to 0) \tag{3.29}$$

From this expression, at the short-time limit, the c.m. exhibits a normal Brownian motion with the diffusivity of $D_G = \left\langle \bar{D} \right\rangle /2$. This result is identical to Eq. (2.7) for the original dumbbell model.

To continue the calculation of Eqs.(3.26)-(3.28), we use the eigenvalue λ_n and the eigenfunction $\psi_n(\xi)$ of $\hat{\mathcal{W}}$, which satisfy

$$\hat{\mathcal{W}}\psi_n(\xi) = \lambda_n \psi_n(\xi) \tag{3.30}$$

for $\hat{\mathcal{W}}$. Here, n is just an eigenfunction or eigenvalue number. We also introduce μ_m and $\phi_m(\xi)$, which satisfy

$$\hat{\mathcal{V}}\phi_m(\xi) = \mu_m \phi_m(\xi) \tag{3.31}$$

for $\hat{\mathcal{V}}$. We employ the basis sets of the eigenfunctions of $\hat{\mathcal{W}}$ and $\hat{\mathcal{V}}$ as

$$\int d\xi \psi_m^\dagger(\xi)\psi_n(\xi) = \delta_{mn} \tag{3.32}$$

and

$$\int d\xi \phi_m^\dagger(\xi)\phi_n(\xi) = \delta_{mn}, \tag{3.33}$$

respectively. We can expand the applied function of $e^{-t\hat{\mathcal{W}}}$ in Eq. (3.26) by the eigenfunctions of $\hat{\mathcal{W}}$ and we obtain Eq. (3.26) as a sum of exponential functions as

$$\Phi(t) = \sum_n p_n e^{-\lambda_n t}, \tag{3.34}$$

$$p_n = \int d\xi \Delta D(\xi)\psi_n(\xi) \int d\xi' \psi_n^\dagger(\xi')\Delta D(\xi')P_{\mathrm{eq}}(\xi'). \tag{3.35}$$

We expand the applied function of $e^{-\hat{\mathcal{V}}}$ in Eq. (3.27) by the eigenfunctions of $\hat{\mathcal{V}}$, and expand the eigenfunctions of $\hat{\mathcal{V}}$ by the eigenfunctions of $\hat{\mathcal{W}}$. Thus, we obtain Eq. (3.27) as

$$\Psi(t,s) = \sum_n \sum_m q_{mn} e^{-\mu_m s - \lambda_n t}, \tag{3.36}$$

$$q_{mn} = \int d\xi \Delta D(\xi)\psi_n(\xi) \int d\xi' \phi_m^\dagger(\xi')P_{\mathrm{eq}}(\xi') \int d\xi'' \psi_n^\dagger(\xi'')\Delta D(\xi'')\phi_m(\xi''). \tag{3.37}$$

We can easily calculate Eq. (3.28) by replacing $P_{\mathrm{eq}}(\xi)$ in Eq. (3.37) to $\bar{D}(\xi)P_{\mathrm{eq}}(\xi)$.

$$\Omega(t,s) = \sum_n \sum_m r_{mn} e^{-\mu_m s - \lambda_n t}, \tag{3.38}$$

$$r_{mn} = \int d\xi \Delta D(\xi)\psi_n(\xi) \int d\xi' \phi_m^\dagger(\xi')\bar{D}(\xi)P_{\mathrm{eq}}(\xi') \int d\xi'' \psi_n^\dagger(\xi'')\Delta D(\xi'')\phi_m(\xi''). \tag{3.39}$$

By performing the integral for the sum of exponential function, we can obtain the MSD of the c.m. as

$$\begin{aligned}\left\langle [\boldsymbol{X}_0(t)-\boldsymbol{X}_0(0)]^2 \right\rangle = n\left\langle \bar{D}\right\rangle t - n\alpha\sum_n p_n \frac{\lambda_n t + e^{-\lambda_n t}-1}{\lambda_n^2} \\ + \frac{n\alpha}{2}\sum_n\sum_m \frac{q_{mn}}{\mu_m}\left(\frac{1-e^{-\lambda_n t}}{\lambda_n} - \frac{e^{-\lambda_n t}-e^{-\mu_m t}}{\mu_m-\lambda_n}\right) \\ + 2n\alpha^2\sum_n\sum_m \frac{r_{mn}}{\mu_m\lambda_n}\left(t - \frac{\mu_m^2(1-e^{-\lambda_n t})-\lambda_n^2(1-e^{-\mu_m t})}{\mu_m\lambda_n(\mu_m-\lambda_n)}\right).\end{aligned} \tag{3.40}$$

In the second place, we obtain the end-to-end relaxation $\boldsymbol{X}_1$ and the relaxation modulus analytically. The end-to-end relaxation $\boldsymbol{X}_1$ can be calculated as

$$\langle \boldsymbol{X}_1(t)\cdot\boldsymbol{X}_1(0)\rangle = \frac{n}{\alpha}\left\langle \exp\left[-2\alpha\int_0^t d\tau \bar{D}(\tau)\right]\right\rangle. \tag{3.41}$$

Also, we can calculate the relaxation modulus by substituting each component of Eq. (3.2) to Eq. (2.10) as shown below.

$$G(t) = \frac{k_B T}{V}\left\langle \exp\left[-4\alpha\int_0^t d\tau \bar{D}(\tau)\right]\right\rangle. \tag{3.42}$$

Here, we use the relation $\alpha = n/\left\langle \boldsymbol{X}_1^2\right\rangle = 1/\left\langle X_{1h}^2\right\rangle$, where $h = x, y$. Eqs (3.43) and (3.44) Eq. (3.41) can be calculated in the same way as that of the MSD of the c.m. :

$$\langle \boldsymbol{X}_1(t)\cdot\boldsymbol{X}_1(0)\rangle = \frac{n}{\alpha}\int d\xi e^{-t\hat{\mathcal{W}}}P_{\mathrm{eq}}(\xi). \tag{3.43}$$

From Eq. (3.42), we can obtain the relaxation modulus can be calculated by replacing α in Eq. (3.41) to 2α as

$$G(t) = \frac{k_B T}{V}\int d\xi e^{-t\hat{\mathcal{V}}}P_{\mathrm{eq}}(\xi). \tag{3.44}$$

Eqs (3.43) and (3.44) also can be expanded by eigenmodes as shown below.

$$\langle \boldsymbol{X}_1(t)\cdot\boldsymbol{X}_1(0)\rangle = \frac{n}{\alpha}\sum_n s_n e^{-\lambda_n t}, \tag{3.45}$$

$$s_n = \int d\xi \psi_n(\xi)\int d\xi' \psi_n^\dagger(\xi')P_{\mathrm{eq}}(\xi'), \tag{3.46}$$

and

$$G(t) = \sum_m G_m e^{-\mu_m t}, \tag{3.47}$$

$$G_m = \frac{k_B T}{V}\int d\xi \phi_m(\xi)\int d\xi' \phi_m^\dagger(\xi')P_{\mathrm{eq}}(\xi'). \tag{3.48}$$

From Eqs (3.46) and (3.48), these correlations have multiple exponential relaxation modes unlike those of the original dumbbell model. Eq. (2.13b) can be interpreted as the OUFD, and the similar result has been obtained by Uneyama et al [22].

3.2 Two-state diffusivity model

To proceed further, we employ the TS model as a fluctuating diffusivity model. In this model, the diffusivity fluctuates between the fast state (named f, $D = D_f$) and the slow state (named s, $D = D_s$). we define k_f and k_s as the transition rates for $f \to s$ and $s \to f$, respectively. The master equation of this model is simple as written below.

$$\frac{d}{dt}\begin{pmatrix} P_f(t) \\ P_s(t) \end{pmatrix} = \begin{pmatrix} -k_f & k_s \\ k_f & -k_s \end{pmatrix}\begin{pmatrix} P_f(t) \\ P_s(t) \end{pmatrix}. \tag{3.49}$$

We call the dumbbell model with the TS model as the TS dumbbell model. In this TS dumbbell model, each diffusivity is independent. For the system as a whole, there are four states in total (ff, fs, sf, ss). Eqs (3.26)-(3.28) for the TS dumbbell model can be calculated as shown below. The derivation of the correlation function $\Phi(t)$ is shown in Appendix E. The other correlation functions can be derived in a similar way as $\Phi(t)$.

$$\Phi(t) = (1\ 1\ 1\ 1)\ \Delta\mathcal{D}\ \boldsymbol{\psi}\ e^{-\Lambda t}\ \boldsymbol{\psi}^{-1}\Delta\mathcal{D}\ \boldsymbol{P}_{\rm eq}. \tag{3.50}$$

$$\Psi(t,s) = (1\ 1\ 1\ 1)\ \Delta\mathcal{D}\ \boldsymbol{\psi}\ e^{-\Lambda t}\ \boldsymbol{\psi}^{-1}\Delta\mathcal{D}\ \boldsymbol{\phi}\ e^{-Ms}\ \boldsymbol{\phi}^{-1}\ \boldsymbol{P}_{\rm eq}. \tag{3.51}$$

$$\Omega(t,s) = (1\ 1\ 1\ 1)\ \Delta\mathcal{D}\ \boldsymbol{\psi}\ e^{-\Lambda t}\ \boldsymbol{\psi}^{-1}\Delta\mathcal{D}\ \boldsymbol{\phi}\ e^{-Ms}\ \boldsymbol{\phi}^{-1}\ \bar{\mathcal{D}}\ \boldsymbol{P}_{\rm eq}. \tag{3.52}$$

Here, we define

$$\Delta\mathcal{D} := \begin{pmatrix} \Delta D(ff) & 0 & 0 & 0 \\ 0 & \Delta D(fs) & 0 & 0 \\ 0 & 0 & \Delta D(sf) & 0 \\ 0 & 0 & 0 & \Delta D(ss) \end{pmatrix} = \begin{pmatrix} 0 & 0 & 0 & 0 \\ 0 & D_f - D_s & 0 & 0 \\ 0 & 0 & D_s - D_f & 0 \\ 0 & 0 & 0 & 0 \end{pmatrix}, \tag{3.53}$$

$$\boldsymbol{P}_{\rm eq} := \begin{pmatrix} P_{\rm eq}(ff) \\ P_{\rm eq}(fs) \\ P_{\rm eq}(sf) \\ P_{\rm eq}(ss) \end{pmatrix} = \frac{1}{(k_s+k_f)^2}\begin{pmatrix} k_s k_s \\ k_s k_f \\ k_f k_s \\ k_f k_f \end{pmatrix}, \tag{3.54}$$

$$\bar{\mathcal{D}} := \begin{pmatrix} \bar{D}(ff) & 0 & 0 & 0 \\ 0 & \bar{D}(fs) & 0 & 0 \\ 0 & 0 & \bar{D}(sf) & 0 \\ 0 & 0 & 0 & \bar{D}(ss) \end{pmatrix} = \begin{pmatrix} D_f & 0 & 0 & 0 \\ 0 & \frac{D_f+D_s}{2} & 0 & 0 \\ 0 & 0 & \frac{D_s+D_f}{2} & 0 \\ 0 & 0 & 0 & D_s \end{pmatrix}, \tag{3.55}$$

$$\boldsymbol{\psi} := (\boldsymbol{\psi}_1\ \boldsymbol{\psi}_2\ \boldsymbol{\psi}_3\ \boldsymbol{\psi}_4), \tag{3.56}$$

$$\Lambda := \begin{pmatrix} \lambda_1 & 0 & 0 & 0 \\ 0 & \lambda_2 & 0 & 0 \\ 0 & 0 & \lambda_3 & 0 \\ 0 & 0 & 0 & \lambda_4 \end{pmatrix}, \tag{3.57}$$

$$\boldsymbol{\phi} := (\boldsymbol{\phi}_1\ \boldsymbol{\phi}_2\ \boldsymbol{\phi}_3\ \boldsymbol{\phi}_4), \tag{3.58}$$

$$M := \begin{pmatrix} \mu_1 & 0 & 0 & 0 \\ 0 & \mu_2 & 0 & 0 \\ 0 & 0 & \mu_3 & 0 \\ 0 & 0 & 0 & \mu_4 \end{pmatrix}. \tag{3.59}$$

$\boldsymbol{\psi}$ and $\boldsymbol{\phi}$ are diagonalization matrixes of the transfer matrix $\mathcal{W}$ and $\mathcal{V}$, respectively, i.e., $\boldsymbol{\psi}_j$ is the eigenvector and λ_j is the eigenvalue of $\mathcal{W}$, and $\boldsymbol{\phi}_k$ is the eigenvector and μ_k is the eigenvalue of $\mathcal{V}$. They satisfy

$$\mathcal{W}\boldsymbol{\psi} = \boldsymbol{\psi}\Lambda, \tag{3.60}$$
$$\mathcal{V}\boldsymbol{\phi} = \boldsymbol{\phi}M. \tag{3.61}$$

We use the transition matrix $\mathcal{L}$ and the transfer matrix $\mathcal{W}$ as shown below. The derivation of this transition matrix is in Appendix F.

$$\mathcal{L} := \begin{pmatrix} -2k_f & k_s & k_s & 0 \\ k_f & -k_f - k_s & 0 & k_s \\ k_f & 0 & -k_f - k_s & k_s \\ 0 & k_f & k_f & -2k_f \end{pmatrix}, \tag{3.62}$$
$$-\mathcal{W} := \mathcal{L} - 2\alpha\bar{\mathcal{D}}, \tag{3.63}$$
$$-\mathcal{V} := \mathcal{L} - 4\alpha\bar{\mathcal{D}}. \tag{3.64}$$

By calculating the eigenvector and the eigenfunction of $\mathcal{W}$ and $\mathcal{V}$, we can obtain the MSD of the c.m., the end-to-end relaxation $\boldsymbol{X}_1$ and the relaxation modulus. The expansion coefficient p_n, q_{mn}, r_{mn}, s_n and G_m in Eqs (3.40), (3.46) and (3.48) can be calculated as shown below.

$$p_n = (1\ 1\ 1\ 1)\ \Delta\mathcal{D}\ \boldsymbol{\psi}_n\ \boldsymbol{\psi}_n^\dagger\ \Delta\mathcal{D}\ \boldsymbol{P}_{\text{eq}}. \tag{3.65}$$
$$q_{mn} = (1\ 1\ 1\ 1)\ \Delta\mathcal{D}\ \boldsymbol{\psi}_n\ \boldsymbol{\phi}_m^\dagger\ \boldsymbol{P}_{\text{eq}}\ \boldsymbol{\psi}_n^\dagger\ \Delta\mathcal{D}\ \boldsymbol{\phi}_m. \tag{3.66}$$
$$r_{mn} = (1\ 1\ 1\ 1)\ \Delta\mathcal{D}\ \boldsymbol{\psi}_n\ \boldsymbol{\phi}_m^\dagger\ \bar{\mathcal{D}}\ \boldsymbol{P}_{\text{eq}}\ \boldsymbol{\psi}_n^\dagger\ \Delta\mathcal{D}\ \boldsymbol{\phi}_m. \tag{3.67}$$
$$s_n = (1\ 1\ 1\ 1)\ \boldsymbol{\psi}_n\ \boldsymbol{\psi}_n^\dagger\ \boldsymbol{P}_{\text{eq}}. \tag{3.68}$$
$$G_m = \frac{k_B T}{V}(1\ 1\ 1\ 1)\ \boldsymbol{\phi}_m\ \boldsymbol{\phi}_m^\dagger\ \boldsymbol{P}_{\text{eq}}. \tag{3.69}$$

We choose $\boldsymbol{\psi}_n^\dagger$ and $\boldsymbol{\phi}_m^\dagger$ defined as

$$\begin{pmatrix} \boldsymbol{\psi}_1^\dagger \\ \boldsymbol{\psi}_2^\dagger \\ \boldsymbol{\psi}_3^\dagger \\ \boldsymbol{\psi}_4^\dagger \end{pmatrix} := \boldsymbol{\psi}^{-1}, \tag{3.70}$$
$$\begin{pmatrix} \boldsymbol{\phi}_1^\dagger \\ \boldsymbol{\phi}_2^\dagger \\ \boldsymbol{\phi}_3^\dagger \\ \boldsymbol{\phi}_4^\dagger \end{pmatrix} := \boldsymbol{\phi}^{-1}. \tag{3.71}$$

The eigenvalues of $\mathcal{W}$ are

$$\begin{cases} \lambda_1 = \alpha(D_f + D_s) + k_f + k_s, & \text{(3.72a)} \\ \lambda_2 = \alpha(D_f + D_s) + k_f + k_s, & \text{(3.72b)} \\ \lambda_3 = \alpha(D_f + D_s) + k_f + k_s + \sqrt{\alpha^2(D_f - D_s)^2 + 2\alpha(D_f - D_s)(k_f - k_s) + (k_f + k_s)^2}, & \text{(3.72c)} \\ \lambda_4 = \alpha(D_f + D_s) + k_f + k_s - \sqrt{\alpha^2(D_f - D_s)^2 + 2\alpha(D_f - D_s)(k_f - k_s) + (k_f + k_s)^2}. & \text{(3.72d)} \end{cases}$$

The eigenvalues of $\mathcal{V}$ are

$$\begin{cases} \mu_1 = 2\alpha(D_f + D_s) + k_f + k_s, & (3.73a) \\ \mu_2 = 2\alpha(D_f + D_s) + k_f + k_s, & (3.73b) \\ \mu_3 = 2\alpha(D_f + D_s) + k_f + k_s + \sqrt{4\alpha^2(D_f - D_s)^2 + 4\alpha(D_f - D_s)(k_f - k_s) + (k_f + k_s)^2}, & (3.73c) \\ \mu_4 = 2\alpha(D_f + D_s) + k_f + k_s - \sqrt{4\alpha^2(D_f - D_s)^2 + 4\alpha(D_f - D_s)(k_f - k_s) + (k_f + k_s)^2}. & (3.73d) \end{cases}$$

We can obtain the longest relaxation time of the end-to-end relaxation and the relaxation modulus from these expressions.

Chapter 4

Results

4.1 Comparison with numerical simulations

To confirm the theoretical calculation results shown in Eq. (3.25), we performed numerical simulations of the TS dumbbell model. We compare the theoretical calculation results of the MSD of the c.m. and the end-to-end relaxation with those of the simulation results. This simulation integrated Eqs. (2.12) for the diffusivity assumed in the TS model with a discrete time δt, and calculated the position of the c.m. and the bond vector. At each time step, the updates of the position and the diffusivity were performed independently from each other. The update for the position was calculated by the stochastic Runge-Kutta method [28], which is the Euler type method introduced for stochastic processes. The update for the diffusivity is calculated exactly to satisfy the transition of Eq. (3.49) for each bead. $D_1(t)$ and $D_2(t)$ flip between D_f and D_s along with the transition possibility derived in Appendix F. From these updating methods, the error for each update is estimated as $\mathcal{O}(\delta t^2)$. The simulation created N_t data points, and we took the average over the data points to calculate the statistical values. We set $\delta t = 0.001$ and $N_t = 10^7$. The other parameters of the TS model is set at $D_f = 5.0$, $D_s = 0.0$, $\alpha = 3$ and $n = 3$.

Fig. 4.1 shows the calculation result for the theoretical calculations and the numerical simulation results with the same parameters. Fig. 4.1(a) shows the agreement of the MSD of the c.m. between the theoretical calculation and the numerical simulation result. In Fig. 4.1(b), the simulation results deviate from the theoretical curves in the long time region due to poor statistics in this time range. Nevertheless, the theory reasonably reproduces the numerical results.

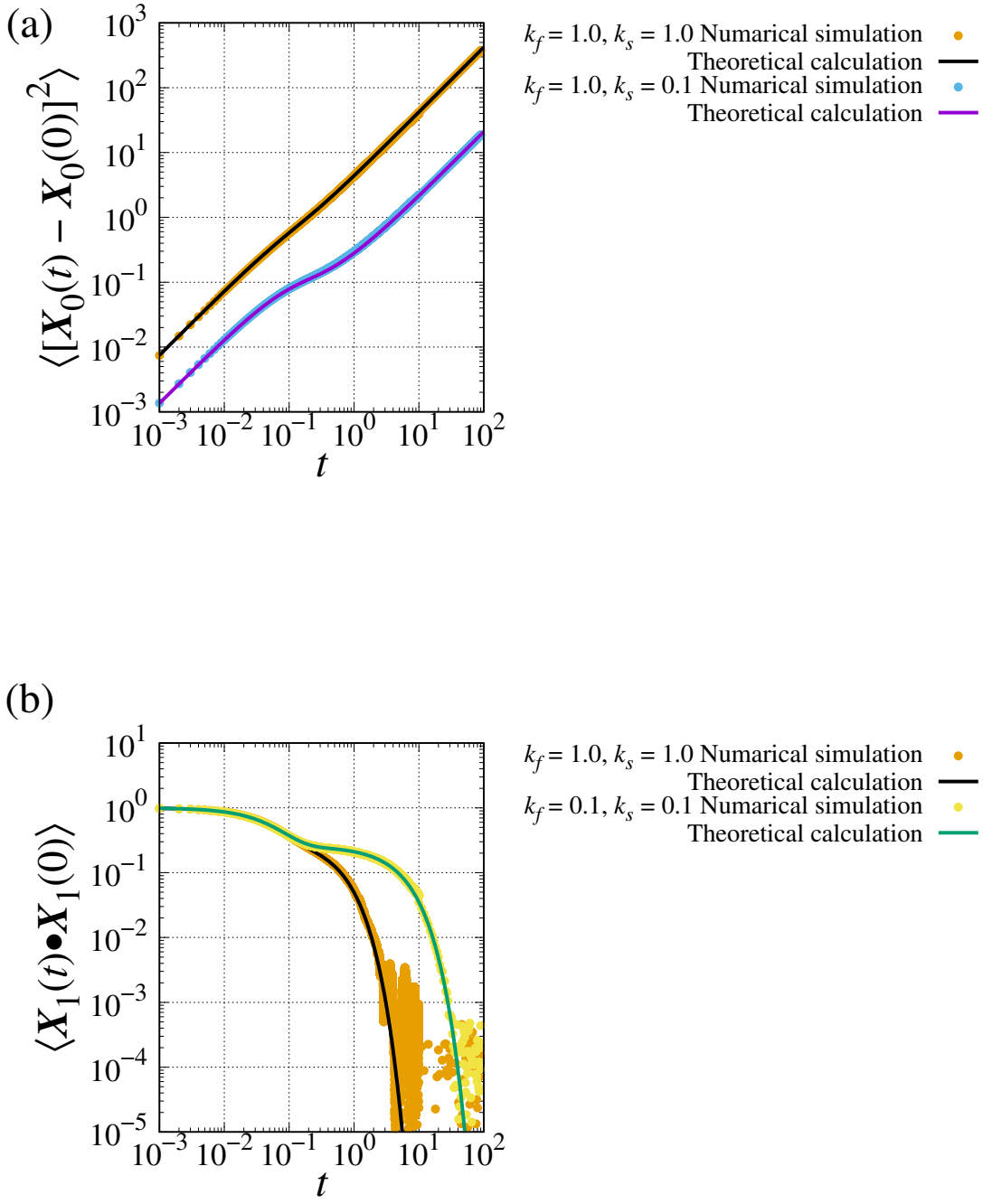

Figure 4.1: Comparison of the MSD of the c.m. (a) and the end-to-end relaxation (b) between theoretical calculation and numerical simulation with various parameters. We set the other parameters as $D_f = 5.0$, $D_s = 0.0$, $\alpha = 3$ and $n = 3$.

4.2 Calculations for some parameters

In this section, owing to the validation of the theory in the previous section, we show some typical calculation results with some sets of parameters. We employ the TS model as the FD model. We compare the MSD of the c.m. and the end-to-end relaxation between the TS dumbbell model and the original dumbbell model. We obtain the values of the original dumbbell model by substituting the average of the diffusivity in the TS model into Eqs (2.7) and (2.8). Since the relaxation modulus is almost the same as the end-to-end relaxation as seen in Eqs (3.43) and (3.44), we omit the result of the relaxation modulus. The eigenvector and the eigenvalue of the transfer matrixes are numerically calculated. We choose a unit of length, time, and mass as $t_0 = \bar{Q}^2/D_f$, $r_0 = \bar{Q}$ and $m_0 = k_B T \bar{Q}^2/D_f^2$, respectively. We set the spatial dimension as $n = 3$. We fix the other parameters as $D_f = 1$, $\bar{Q} = 1$, and $V = \bar{Q}^3$. Thus, the characteristic values are D_s/D_f, and k_f and k_s.

In Fig. 4.2 to Fig. 4.4, we show the effects of the transition rates. Fig. 4.2 shows the entire match between the calculation results of the TS dumbbell and those of the original dumbbell for $k_f = 100$. From Fig. 4.2, the MSD of c.m. and the end-to-end relaxation converge to those of the original dumbbell model with the high transition rates. In Fig. 4.3, k_f value is reduced from 100 to 1. In Fig. 4.3(a), the sub-diffusion of the MSD can be observed when the ratio between the transition rates k_s/k_f becomes small. The ratio also affects the relaxation time of the end-to-end relaxation as seen in Fig. 4.3(b). The deviation from the original dumbbell becomes significant for the small k_s/k_f values. In Fig. 4.4, k_f is further reduced to 10^{-3}. From Fig. 4.4(a), for this case, the sub-diffusion in the MSD becomes more apparent and the transitional region is elongated when k_s/k_f ratio becomes small. Fig. 4.4(b) demonstrates that the deviation from the original dumbbell is enhanced. Further, for the case of $k_s/k_f = 1$, a two-step relaxation is observed.

From Fig. 4.4(a), the plateau range of the MSD is observed from the transition rate and the low these ratios. Also, we can observe the definite multi-mode relaxation in Fig. 4.4(b) with the low transition rate and $k_s/k_f = 1$.

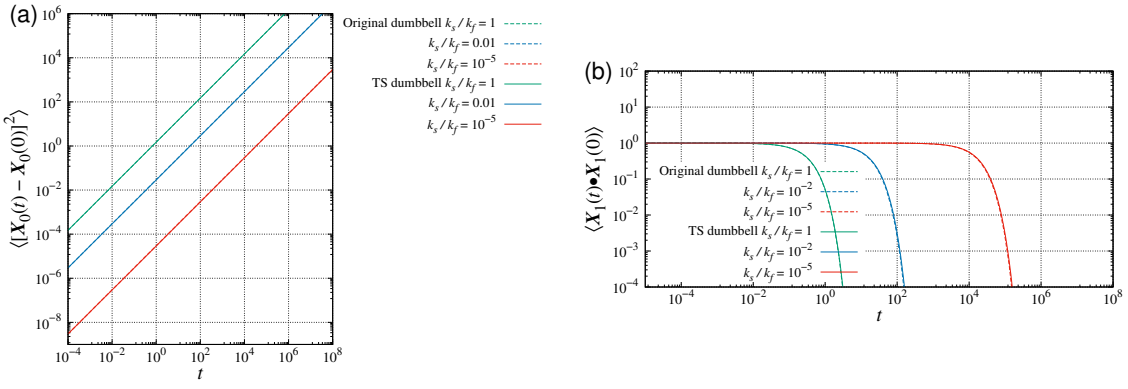

Figure 4.2: MSD (a) and end-to-end relaxation (b) of the TS dumbbell model for $k_f = 100$, $D_s = 0$ and $D_f = 1$ with various k_s values. The solid curves represent the theoretical calculation in the TS dumbbell model. The prediction of the original dumbbell model is shown by dashed curves. The values of the original dumbbell model are obtained from Eqs (2.7) and (2.8) with the average of the diffusivity. The results for both models are completely matched with each other.

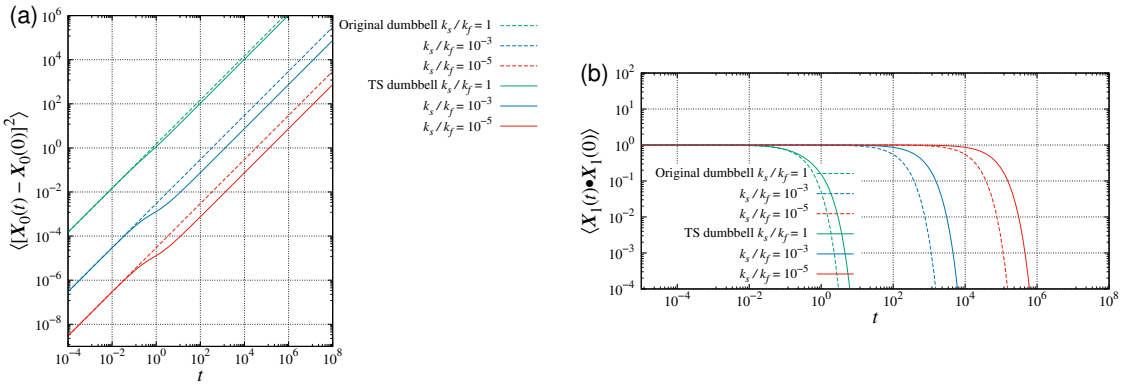

Figure 4.3: MSD (a) and end-to-end relaxation (b) of the TS dumbbell model for $k_f = 1$, $D_s = 0$ and $D_f = 1$ with various k_s values. The solid curves represent the theoretical calculation in the TS dumbbell model. The prediction of the original dumbbell model is shown by dashed curves. The values of the original dumbbell model are obtained from Eqs (2.7) and (2.8) with the average of the diffusivity.

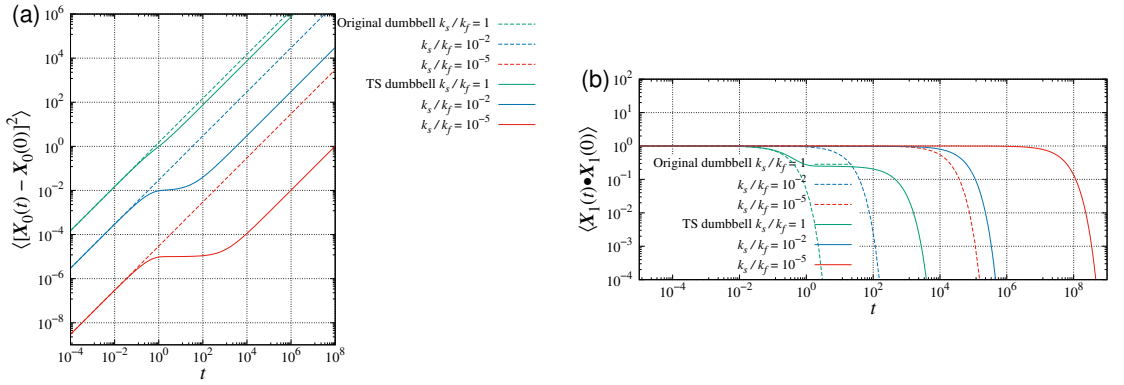

Figure 4.4: MSD (a) and end-to-end relaxation (b) of the TS dumbbell model for $k_f = 10^{-3}$, $D_s = 0$ and $D_f = 1$ with various k_s values. The solid curves represent the theoretical calculation in the TS dumbbell model. The prediction of the original dumbbell model is shown by dashed curves. The values of the original dumbbell model are obtained from Eqs (2.7) and (2.8) with the average of the diffusivity.

In Fig. 4.5, we show the effect of the diffusivities. Here, we choose $k_f = 10^{-3}$ and $k_s = 10^{-8}$ to observe the sub-diffusion. For both of the MSD (Panel (a)) and the end-to-end relaxation (Panel (b)), the deviations from the original dumbbell become larger with the smaller D_s. This result is rational because the deviations come from the difference of the diffusivities as seen in Eqs (3.25) and (3.43). Note that the result approaches to those of the original dumbbell when $D_f \to D_s$.

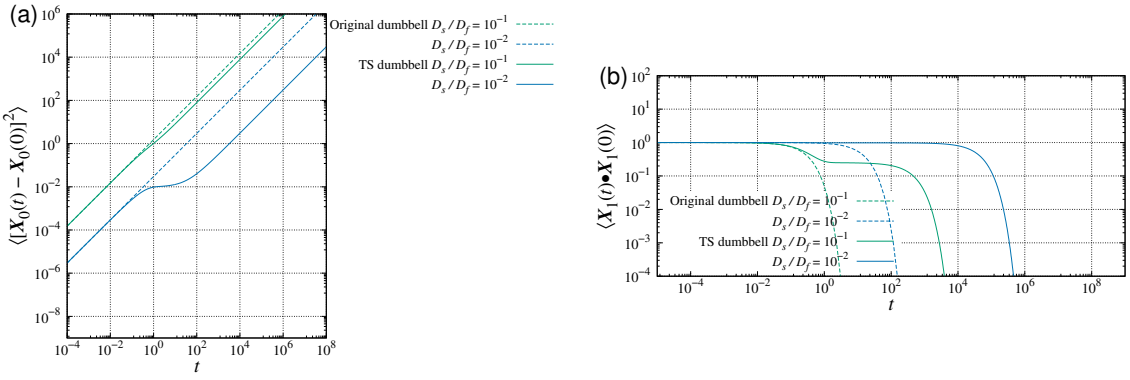

Figure 4.5: MSD (a) and end-to-end relaxation (b) of the TS dumbbell model for $k_f = 10^{-3}$, $k_s = 10^{-8}$ and $D_f = 1$ with various D_s values. The solid curves represent the theoretical calculation in the TS dumbbell model. The prediction of the original dumbbell model is shown by dashed curves. The values of the original dumbbell model are obtained from Eqs (2.7) and (2.8) with the average of the diffusivity.

Chapter 5

Discussion

5.1 Comparison with original dumbbell model

In this section, we discuss the differences between the FD dumbbell model and the original Hookean dumbbell model based on the results of the TS dumbbell model shown in the previous section.

Let us start with the effect of the state transition. From Fig. 4.2, the MSD of the c.m. and the correlation functions (the end-to-end relaxation and the relaxation modulus) of the TS dumbbell converge to those of the original dumbbell model. At the limit of large transition rates, the eigenvalues of the transition matrix $\mathcal{L}$ become large, and the transition between the states proceeds fast. Thus the average value of the diffusivity becomes dominant. Similarly, with the general FD model, if the state relaxation is fast, the results of the FD dumbbell converge to those of the original dumbbell model.

When the state relaxation is not so fast, the effect of the FD appears like Fig. 4.3. From (3.25), the integral including $\Phi(t)$ will be dominant at the long time range. We can estimate the time range of the sub-diffusion from the integral in Eq. (3.40). By expanding $e^{-\lambda_n t}$, we can estimate that the sub-diffusion starts at the time when the $(\lambda_n t)^2$ term cannot be ignored. In other words, the sub-diffusion starts at the $1/\lambda_{\max}$, where the $\lambda_{\max}$ is the maximum eigenvalue.

The effect of the difference of the diffusivities is clear. Since the sub-diffusion is caused by the difference of the diffusivities, the size of the deviation from the original dumbbell model obeys the size of the difference between D_f and D_s. More generally, the magnitude of the fluctuation of the diffusivity also decides the deviation from the original dumbbell model.

5.2 Comparison with molecular simulations

Comparison with glassy polymer melt

From the results shown above, the c.m. of the TS dumbbell model shows the sub-diffusion with specific parameters. Thus, it may be able to describe the dynamics of polymers in heterogeneous environments. In this section, we discuss simulation results of the supercooled or glassy melt by the TS dumbbell model.

In glassy unentangled polymer melts at high temperatures, the MSD of the c.m. crosses over from the ballistic range to the diffusion range directly. Besides, at low temperatures, the MSD of the c.m. has a plateau range between the ballistic range and the diffusion range.

Since the TS model is the model that regards the dynamic heterogeneity in glassy systems as two-state fluctuating diffusivity [23, 19], it is likely to describe the dynamics in the supercooled liquids. With this idea, we use the TS dumbbell model for the description of the dynamics of the supercooled polymer melts. We assume that the fluctuating process can be regarded as the Markovian TS model.

Note that the ergodicity is broken in the glassy condition and we cannot use the dumbbell theory, which is established with the equilibrium statistical mechanics for those systems. We apply the TS dumbbell model for the supercooled liquids with the assumption that the system is in the equilibrium state but a quasi-equilibrium state.

We compare the TS dumbbell model for the results of molecular dynamics simulations, which were performed by Bennemann et al. [29]. In the study, polymers are described as a series of beads that are connected by springs. The beads interact with each other through a Lennard-Jones (LJ) potential

$$U_{\mathrm{LJ}}(\boldsymbol{r}_{jk}) = 4\epsilon \left[\left(\frac{\sigma}{|\boldsymbol{r}_{jk}|} \right)^{12} - \left(\frac{\sigma}{|\boldsymbol{r}_{jk}|} \right)^{6} \right], \tag{5.1}$$

where $\boldsymbol{r}_{jk}$ is the relative vector defined as $\boldsymbol{r}_{jk} = \boldsymbol{R}_j - \boldsymbol{R}_k$. In the simulation, LJ potential is cut off at $2 \times 2^{\frac{1}{6}}\sigma$ and shifted up so that the potential is continuous at the cut point shown as shown below.

$$U_{\mathrm{LJ}}(\boldsymbol{r}_{jk}) = \begin{cases} 4\epsilon \left[\left(\frac{\sigma}{|\boldsymbol{r}_{jk}|} \right)^{12} - \left(\frac{\sigma}{|\boldsymbol{r}_{jk}|} \right)^{6} + \frac{2^7-1}{2^{14}} \right] & (|\boldsymbol{r}_{jk}| \leq 2 \times 2^{\frac{1}{6}}\sigma) \\ 0 & (2 \times 2^{\frac{1}{6}}\sigma < |\boldsymbol{r}_{jk}|) \end{cases} \tag{5.2}$$

ϵ and σ are correspond to the magnitude and the width of the LJ potential, respectively, The unit energy is set at ϵ, and the unit length is set at σ. The potential of the spring is described by the FENE potential :

$$U_{\mathrm{FENE}}(\boldsymbol{r}_{jk}) = -15R_0^2 \ln \left[1 - \left(\frac{|\boldsymbol{r}_{jk}|}{R_0} \right) \right] \tag{5.3}$$

with $R_0 = 1.6$. This potential works only for the neighboring beads. The total equilibrium length l_0 is $l_0 = 0.96$. The number of beads is chosen as $N = 10$, which does not show the entangle effects. This simulation is performed in the canonical (NVT) ensemble using the Nose–Hoover thermostat. The equilibrium density is calculated by the NPT simulation before the NVT simulation.

We fit the expression of Eq. (3.25) of the TS dumbbell model. We set the unit of length as σ, the unit of energy as k_BT and the unit of mass as the mass of the Lennard-Jones particle. The fitting parameters are D_f, k_f and k_s. D_s and α are fixed as $D_s = 0.0$, $\alpha = 3.0$ and $n = 3$. We assume $D_s = 0.0$ because the dynamics of the bead is strongly restricted at slow state and we assume the diffusivity as zero.

Fig. 5.1 shows the results of fitting for the temperature $T = 1$ and $T = 0.48$. Table 5.1 shows the fitting parameters. Since the Langevin equations of the FD dumbbell are over-dumped type and do not contain inertia terms, we ignore the values in the ballistic range. We confirm that the TS dumbbell can describe the anomalous diffusion in this glassy polymer melt.

Table 5.1: The fitting parameters for the result of the simulation for the glassy polymer melts[29]. The other parameters are fixed at $D_s = 0, \alpha = 3, n = 3$.

T	D_f	k_f	k_s
1	3.4×10^{-2}	4.1×10^{-4}	4.1×10^{-4}
0.48	4.6×10^{-1}	1.6×10^{-4}	1.8×10^{-6}

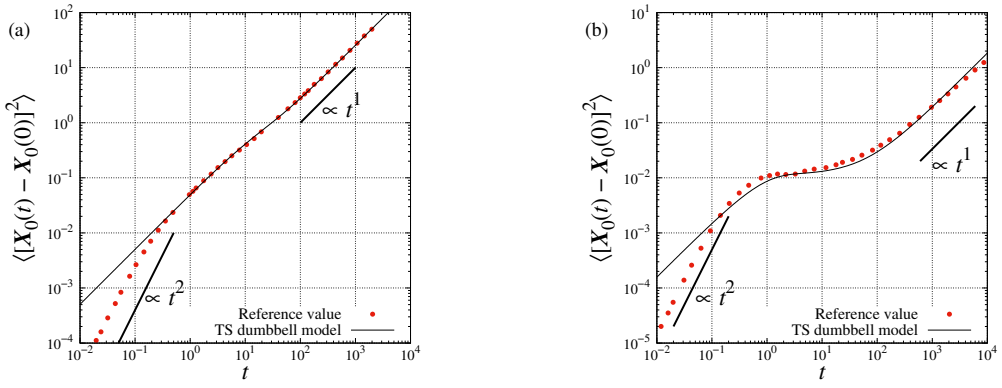

Figure 5.1: Comparison of the MSD of the MD simulation [29] with that of the TS dumbbell model predictions at (a)$T = 1$ and (b)$T = 0.48$. The fitting parameters are shown in Fig. 5.1. The unit of length, energy, and mass are set at the same as the molecular simulations.

From the parameters in Table 5.1, we can estimate the condition of the dynamics of the polymers. From Eq. (3.49), we can calculate the steady possibility for the state f and the state s. We call them as P_f and P_s, respectively. They can be calculated as shown below.

$$P_f = \frac{k_s}{k_f + k_s}, \tag{5.4}$$

$$P_s = \frac{k_f}{k_f + k_s}. \tag{5.5}$$

By calculating these values from the result in Table 5.1, we obtain P_f and P_s in Table 5.2. From Table 5.2, we can see that in the weak glassy state at $T = 1$, the state possibilities are almost the same. It means that the beads of the dumbbell can take any states, and the mobility restriction is weak. Besides, in the strong glassy state at $T = 0.48$, the possibility of s state is dominant. This means that the beads are restricted in s state and the mobility restriction is very strong in the state. This result agrees with the physical picture of the glassy state, where the mobility restriction of the slow range is so strong that the beads cannot move freely. The steady possibilities for the dumbbell itself also can be calculated from Eq. (3.54). The result is almost the same as that of the single Brownian bead.

Table 5.2: Steady possibilities for each state calculated by the fitting parameters. They are obtained from Eq. (5.5). The parameters in Eq. (5.5) are shown in Table 5.1.

T	P_f	P_s
1	5.0×10^{-1}	5.0×10^{-1}
0.48	1.1×10^{-2}	9.9×10^{-1}

However, the relaxation behavior of the TS dumbbell model is different from that of the simulation result or real systems. In the supercooled polymer melt, the relaxation function is the stretched-exponential function (KWW type), which have t^β factor in the exponential argument [29]. β is the KWW index with $0 < \beta < 1$. The relaxation functions of the Markovian FD dumbbell model are multiple exponential functions with any FD models, and the FD dumbbell cannot describe the KWW type decay in principle.

The non-Markovian OUFD has been developed by Miyaguchi et al [30]. With the non-equilibrium waiting time distribution, the relaxation function of the OUFD exhibits the KWW type relaxation. Thus, if the fluctuation of the diffusivity in the TS dumbbell model is non-Markovian, it also may be able to describe the KWW type relaxation. For the non-Markovian process, we cannot use the theory of the transfer operator. The TS model with the limit of $D_f \to \infty$, $D_s = 0$ can be regarded as the CTRW model, and a similar calculation can be applied for the non-Markovian processes. To calculate the non-Markovian TS dumbbell, we have to use the theory of the CTRW.

Comparison with entangled polymer melt

In this section, we attempt to compare the TS dumbbell model to the simulation result of the entangled polymer melts. We assume that the movement of the entangled point is restricted, and the diffusivity is small. With this rough picture, the TS dumbbell model may describe the dynamics of the entangled polymer melts, by assuming the diffusivity of the unentangled point as fast, and that of the entangled point as slow.

We apply the TS dumbbell model for the results of a coarse-grained model, which was developed by Uneyama et al. [31]. The slip-spring model [32] is one of the coarse-grained models for entangled polymers, in which the polymer is connected with the other spring. This spring is called slip-spring, and the other end is fixed at space, and the other end can slide on the polymer chain. This model can describe the diffusion and rheological behaviors of entangled polymers well.

We performed the fitting with fitting function Eq. (3.25) with the TS model. We choose the rescaling parameter as 0.1 for the time axis and 0.1 for the MSD axis. With these parameters, we fixed the values of the simulation results. The fitting parameters were D_f, D_s, and k_f. The other parameters were fixed as $k_s = 1.6 \times 10^{-2}$, $\alpha = 3.0$ and $n = 3$.

Fig. 5.2 shows the comparison between the MSD of the c.m. of the TS dumbbell model and that of the slip-spring simulation with the number of beads $N = 10, 20$. Table 5.3 shows the calculated fitting parameters.

Table 5.3: Fitting parameters for entangled polymer simulation[31]. The other parameters are fixed as $k_s = 1.6 \times 10^{-2}$, $\alpha = 3.0$ and $n = 3$.

N	Df	Ds	k_f
10	8.9×10^{-2}	9.5×10^{-2}	1.0×10^{-1}
20	2.8×10^{-1}	6.6×10^{-3}	7.8×10^{-2}

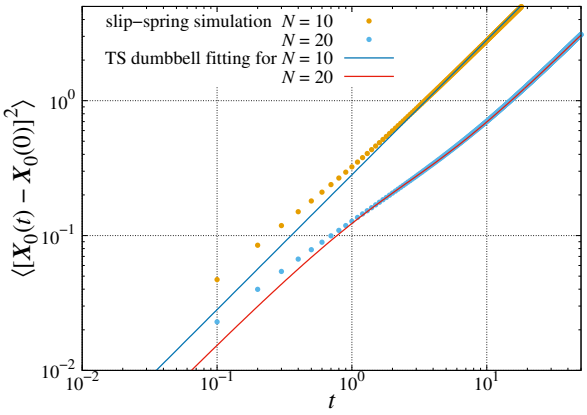

Figure 5.2: Fitting result for entangled polymer simulation. The unit time of the TS dumbbell model is 10 times that of the simulation, and the unit length is $\sqrt{10}$ times that of the simulation.

The TS dumbbell model cannot reproduce the results of the slip-spring simulation in the short time range as seen in Fig. 5.2. There are some reasons for this result. First, at least with the TS model, the form of expression in Eq. (3.25) cannot show the form of diffusion behavior [31] for entangled polymers as

$$\left\langle [\boldsymbol{X}_0(t) - \boldsymbol{X}_0(0)]^2 \right\rangle \propto \begin{cases} t & (t \lesssim \tau_e), \\ t^{1/2} & (\tau_e \lesssim t \lesssim \tau_R), \\ t & (t \lesssim \tau_R), \end{cases} \tag{5.6}$$

where τ_e is the entanglement time, and τ_R is the Rouse time of the entangled polymer. Eq. (3.25) with the TS model does not have a long time $\propto t^{1/2}$ dependency. We consider the reason as the lack of relaxation modes in Eqs.(3.26)-(3.28). The OUFD with the DD model, which is a continuous FD model has the $\propto t^{-1/2}$ dependency in the relaxation function. The FD dumbbell with such a continuous FD model may exhibit the $\propto t^{1/2}$ dependency from the similar mechanism.

Moreover, the dumbbell estimation may be too rough to describe the entangled polymers. If we assume a condition that the polymer is in a homogeneous state, the diffusivity may not fluctuate. The polymers in such liquids exhibit multiple relaxation modes. Meanwhile, that of the FD dumbbell without the fluctuation of the diffusivity naturally exhibits the single relaxation behavior. To solve this contradiction, introducing the FD to the Rouse model [3] may be effective. The Rouse model is a coarse-grained model for polymers which regard the polymer as the many Brownian beads connected by the Hookean spring. The Rouse model also exhibits the multiple relaxation modes due to the number of the configuration modes. We may be able to describe the dynamics of polymers in heterogeneous environments by using the Rouse model with the FD, and to describe that of polymers in homogeneous environments comprehensively by weakening the fluctuation of the diffusivity. Also, by introducing the FD to the Rouse model, we can describe the more detailed fluctuation of the diffusivities for each bead (or each position), and it seems to be physically reasonable model for polymers.

Chapter 6

Conclusion

In this work, we introduced the FD model to the Hookean dumbbell model and calculated the MSD of the c.m., the end-to-end relaxation, and the relaxation modulus analytically. The characteristic feature of the FD dumbbell model is that the diffusivities of dumbbell beads are not common.

For the analytical calculation, we described the ensembled average derived from solutions of the Langevin equations as the average of the state path function. We used the discrete time for the path function. Under the assumption of the Markovian process of the path function, we calculated the integrands of the MSD of the c.m. As a result, the c.m. of the FD dumbbell model exhibits the sub-diffusion with the characteristic time of eigenvalues of the transfer operator. Also, the end-to-end relaxation and the relaxation modulus have the multiple relaxation modes with the characteristic time.

To confirm the theoretical calculations, we performed the numerical simulations of the TS dumbbell model. The result is in excellent agreement with the theoretical calculation. From this result, the theoretical calculation is validated.

We used the TS dumbbell model to describe the anomalous diffusion in the unentangled supercooled polymer melt. We fit the parameters of the TS dumbbell to the weak supercooled state with a relatively high transition rate and the strongly supercooled state with the relatively low transition rate. This result may suggest the mobility restriction in the supercooled liquid. However, the correlation functions do not show the KWW type relaxation as long as the fluctuating process of the diffusivity is Markovian.

We also attempted to describe the anomalous diffusion in the entangled polymer melt by the TS dumbbell model. The TS dumbbell cannot reproduce the results of the simulation. This may be mainly because of the lack of beads number or lack of states. Also, characteristic relaxation times of the FD dumbbell model and entangled polymer are different from each other. Thus, the FD dumbbell model may be not good model to describe the dynamics of the entangled polymer.

From the results mentioned above, the FD dumbbell model is the minimum model to describe the diffusion dynamics of polymers in heterogeneous environments. There are some conceivable solutions for the defect of the TS or FD dumbbell model. One of them is replacing the Markovian FD with the non-Markovian FD for the description of the glassy polymer. The dumbbell model with non-Markovian FD may describe the KWW type relaxation because the non-Markovian OUFD exhibits KWW type relaxation. The other solution is introducing the other FD model instead of the TS model, and another is introducing the FD to the Rouse model. The reason for that the TS dumbbell model cannot describe the dynamics of the entangled polymer is considered to be the lack of relaxation modes. By using the other FD model which has infinite states, we

can obtain infinite relaxation modes due to the number of the states. Also, by introducing the FD model to the Rouse model, we can obtain almost infinite relaxation modes due to the number of the configuration modes.

Acknowledgments

本卒業論文の執筆にあたり，多くの方々のお力添えを賜りました．

増渕雄一教授には，本研究室での研究の機会を与えてくださり，一貫してご指導を賜りました．ゼミ発表や，個別でご相談させていただくたびに多くのご助言をくださり，終始楽しく研究に打ち込むことができました．心より感謝申し上げます．

畝山多加志准教授には，研究の基礎事項や応用的な内容まで，本研究の内容のみに留まらず，多くのことをご教授いただきました．他分野の知識も多く得ることができ，非常に有意義な 1 年を過ごすことができました．改めてお礼申し上げます．

土肥侑也助教，木田拓充特任助教におかれましては，幾度も研究内容に関するご相談にお付き合いいただきました．実験的な立場からのご助言は私にとってとても有益で，常に実験系を意識して研究を進めることができました．深く感謝申し上げます．

また，研究室の先輩方には，研究から日常生活まで，様々なことについてご相談に乗っていただきました．この 1 年間は私にとって初めてのことばかりでしたが，先輩方の親身なご指導あってこそ，乗り越えることができました．同期達とも切磋琢磨し，また支え合いながら楽しく過ごせた 1 年間でした．ありがとうございました．

最後に，私の大学生活を支え，見守って下さった家族に心からお礼申し上げます．

Appendix

A Detail calculation of MSD in FD dumbbell model

In this appendix, we show the detail calculations from Eq. (3.3) to Eq. (3.4).

By substituting Eq. (3.2) to Eq. (3.3), we have

$$\begin{aligned}\left\langle \Delta D(\tau)\boldsymbol{X}_1(\tau)\cdot\bar{\boldsymbol{\Xi}}(\tau')\right\rangle =& \left\langle \Delta D(\tau)\exp\left[-2\alpha\int_0^\tau d\upsilon\bar{D}(\upsilon)\right]\boldsymbol{X}_1(0)\cdot\bar{\boldsymbol{\Xi}}(\tau')\right\rangle \\ &+\int_0^\tau d\upsilon\left\langle \Delta D(\tau)\exp\left[-2\alpha\int_\upsilon^\tau d\upsilon'\bar{D}(\upsilon')\right]\Delta\boldsymbol{\Xi}(\upsilon)\cdot\bar{\boldsymbol{\Xi}}(\tau')\right\rangle \\ =&\int_0^\tau d\upsilon\left\langle \Delta D(\tau)\exp\left[-2\alpha\int_\upsilon^\tau d\upsilon'\bar{D}(\upsilon')\right]\Delta\boldsymbol{\Xi}(\upsilon)\cdot\bar{\boldsymbol{\Xi}}(\tau')\right\rangle \\ =&n\int_0^\tau d\upsilon\left\langle \Delta D(\tau)\exp\left[-2\alpha\int_\upsilon^\tau d\upsilon'\bar{D}(\upsilon')\right]\Delta D(\tau')\delta(\upsilon-\tau')\right\rangle .\end{aligned} \tag{A.1}$$

From Eq. (2.22), for the case $0<\tau'<\tau$,

$$\left\langle \Delta D(\tau)\boldsymbol{X}_1(\tau)\cdot\bar{\boldsymbol{\Xi}}(\tau')\right\rangle = n\left\langle \Delta D(\tau)\exp\left[-2\alpha\int_{\tau'}^\tau d\upsilon'\bar{D}(\upsilon')\right]\Delta D(\tau')\right\rangle , \tag{A.2}$$

and for the case $\tau<\tau'$, $\left\langle \Delta D(\tau)\boldsymbol{X}_1(\tau)\cdot\bar{\boldsymbol{\Xi}}(\tau')\right\rangle = 0$. Thus, we have

$$\int_0^t d\tau\int_0^t d\tau'\left\langle \Delta D(\tau)\boldsymbol{X}_1(\tau)\cdot\bar{\boldsymbol{\Xi}}(\tau')\right\rangle = n\int_0^t d\tau\int_0^\tau d\tau'\left\langle \Delta D(\tau)\exp\left[-2\alpha\int_{\tau'}^\tau d\upsilon\bar{D}(\upsilon)\right]\Delta D(\tau')\right\rangle . \tag{A.3}$$

Also, we have

$$
\begin{aligned}
&\left\langle \Delta D(\tau)\Delta D(\tau')\boldsymbol{X}_1(\tau)\cdot\boldsymbol{X}_1(\tau')\right\rangle \\
=&\left\langle \Delta D(\tau)\Delta D(\tau')\exp\left[-2\alpha\int_0^{\tau}d\upsilon\bar{D}(\upsilon)-2\alpha\int_0^{\tau'}d\upsilon'\bar{D}(\upsilon')\right]\boldsymbol{X}_1^2(0)\right\rangle \\
&+2\int_0^{\tau}ds\left\langle \Delta D(\tau)\Delta D(\tau')\exp\left[-2\alpha\int_0^{\tau}d\upsilon\bar{D}(\upsilon)-2\alpha\int_s^{\tau'}d\upsilon'\bar{D}(\upsilon')\right]\boldsymbol{X}_1(0)\cdot\Delta\boldsymbol{\Xi}(s)\right\rangle \\
&+\int_0^{\tau}ds\int_0^{\tau'}ds'\left\langle \Delta D(\tau)\Delta D(\tau')\exp\left[-2\alpha\int_s^{\tau}d\upsilon\bar{D}(\upsilon)-2\alpha\int_{s'}^{\tau'}d\upsilon'\bar{D}(\upsilon')\right]\Delta\boldsymbol{\Xi}(s)\cdot\Delta\boldsymbol{\Xi}(s')\right\rangle \\
=&\frac{n}{\alpha}\left\langle \Delta D(\tau)\Delta D(\tau')\exp\left[-2\alpha\int_0^{\tau}d\upsilon\bar{D}(\upsilon)-2\alpha\int_0^{\tau'}d\upsilon'\bar{D}(\upsilon')\right]\right\rangle \\
&+0 \\
&+4n\int_0^{\tau}ds\int_0^{\tau'}ds'\left\langle \Delta D(\tau)\Delta D(\tau')\exp\left[-2\alpha\int_s^{\tau}d\upsilon\bar{D}(\upsilon)-2\alpha\int_{s'}^{\tau'}d\upsilon'\bar{D}(\upsilon')\right]\bar{D}(s)\delta(s-s')\right\rangle \\
=&\frac{n}{\alpha}\left\langle \Delta D(\tau)\Delta D(\tau')\exp\left[-2\alpha\int_0^{\tau}d\upsilon\bar{D}(\upsilon)-2\alpha\int_0^{\tau'}d\upsilon'\bar{D}(\upsilon')\right]\right\rangle \\
&+4n\int_0^{\min(\tau,\tau')}ds\left\langle \Delta D(\tau)\Delta D(\tau')\exp\left[-2\alpha\int_s^{\tau}d\upsilon\bar{D}(\upsilon)-2\alpha\int_s^{\tau'}d\upsilon'\bar{D}(\upsilon')\right]\bar{D}(s)\right\rangle .
\end{aligned}
\tag{A.4}
$$

With Eq. (A.2) and Eq. (A.4), we can rewrite Eq. (3.3) as

$$
\begin{aligned}
&\left\langle[\boldsymbol{X}_0(t)-\boldsymbol{X}_0(0)]^2\right\rangle-n\left\langle\bar{D}\right\rangle t \\
=&-\alpha\int_0^t d\tau\int_0^t d\tau'\left\langle\Delta D(\tau)\boldsymbol{X}_1(\tau)\cdot\bar{\boldsymbol{\Xi}}(\tau')\right\rangle \\
&+\frac{\alpha^2}{4}\int_0^t d\tau\int_0^t d\tau'\left\langle\Delta D(\tau)\Delta D(\tau')\boldsymbol{X}_1(\tau)\cdot\boldsymbol{X}_1(\tau')\right\rangle \\
=&-\alpha\int_0^t d\tau\int_0^{\tau}d\tau'\left\langle\Delta D(\tau)\exp\left[-2\alpha\int_{\tau'}^{\tau}d\upsilon\bar{D}(\upsilon)\right]\Delta D(\tau')\right\rangle \\
&+\frac{n\alpha}{4}\int_0^t d\tau\int_0^t d\tau'\left\langle\Delta D(\tau)\Delta D(\tau')\exp\left[-2\alpha\int_0^{\tau}d\upsilon\bar{D}(\upsilon)-2\alpha\int_0^{\tau'}d\upsilon'\bar{D}(\upsilon')\right]\right\rangle \\
&+n\alpha^2\int_0^t d\tau\int_0^t d\tau'\int_0^{\min(\tau,\tau')}d\tau''\left\langle\Delta D(\tau)\Delta D(\tau')\exp\left[-2\alpha\int_s^{\tau}d\upsilon\bar{D}(\upsilon)-2\alpha\int_s^{\tau'}d\upsilon'\bar{D}(\upsilon')\right]\bar{D}(\tau'')\right\rangle \\
=&-\alpha\int_0^t d\tau\int_0^{\tau}d\tau'\left\langle\Delta D(\tau)\exp\left[-2\alpha\int_{\tau'}^{\tau}d\upsilon\bar{D}(\upsilon)\right]\Delta D(\tau')\right\rangle \\
&+\frac{n\alpha}{2}\int_0^t d\tau\int_0^{\tau}d\tau'\left\langle\Delta D(\tau)\Delta D(\tau')\exp\left[-2\alpha\int_0^{\tau}d\upsilon\bar{D}(\upsilon)-2\alpha\int_0^{\tau'}d\upsilon'\bar{D}(\upsilon')\right]\right\rangle \\
&+2n\alpha^2\int_0^t d\tau\int_0^{\tau}d\tau'\int_0^{\tau'}d\tau''\left\langle\Delta D(\tau)\Delta D(\tau')\exp\left[-2\alpha\int_s^{\tau}d\upsilon\bar{D}(\upsilon)-2\alpha\int_s^{\tau'}d\upsilon'\bar{D}(\upsilon')\right]\bar{D}(\tau'')\right\rangle .
\end{aligned}
\tag{A.5}
$$

B Detail calculation of correlation functions in FD dumbbell model

In this appendix, we show the detail derivations of Eq. (3.20) and Eq. (3.21).

First, we derive Eq. (3.20). In the same way as $\Phi(t)$, Eq. (3.6) can be calculated as

$$
\begin{aligned}
\Psi(t,t') &= \left\langle \Delta D(t)\Delta D(t') \exp\left[-2\alpha\int_0^t d\tau \bar{D}(\tau) - 2\alpha\int_0^{t'} d\tau' \bar{D}(\tau')\right]\right\rangle \\
&= \int \mathcal{D}\xi \Delta D(\xi(t))\Delta D(\xi(t')) \exp\left[-2\alpha\int_0^t d\tau \bar{D}(\xi(\tau)) - 2\alpha\int_0^{t'} d\tau' \bar{D}(\xi(\tau'))\right]\mathcal{P}[\xi] \\
&= \int \mathcal{D}\xi \Delta D(\xi(t)) \exp\left[-2\alpha\int_{t'}^t d\tau \bar{D}(\xi(\tau))\right]\Delta D(\xi(t')) \exp\left[-4\alpha\int_0^{t'} d\tau' \bar{D}(\xi(\tau'))\right]\mathcal{P}[\xi] \\
&\approx \int \prod_{i=0}^{t/\delta t} d\xi_i \Delta D(\xi(t)) \exp\left[-2\alpha\sum_{i=t'/\delta t}^{t/\delta t-1} \delta t \bar{D}(\xi_i)\right]\Delta D(\xi_{t'/\delta t}) \exp\left[-4\alpha\sum_{i=0}^{t'/\delta t-1} \delta t \bar{D}(\xi_i)\right] \\
&\quad \times \exp\left[-\delta t\sum_{i=0}^{t/\delta t-1} s(\xi_{i+1},\xi_i)\right] P(\xi_0) \\
&= \int \prod_{i=0}^{t/\delta t} d\xi_i \Delta D(\xi(t)) \exp\left[-\delta t\sum_{i=t'/\delta t}^{t/\delta t-1} \left\{s(\xi_{i+1},\xi_i) + 2\alpha\bar{D}(\xi_i)\right\}\right]\Delta D(\xi_{t'/\delta t}) \\
&\quad \times \exp\left[-\delta t\sum_{i=0}^{t'/\delta t-1} \left\{s(\xi_{i+1},\xi_i) + 4\alpha\bar{D}(\xi_i)\right\}\right] P(\xi_0) \\
&= \int \prod_{i=t'/\delta t}^{t/\delta t} d\xi_i \Delta D(\xi(t)) \exp\left[-\delta t\sum_{i=t'/\delta t}^{t/\delta t-1} \left\{s(\xi_{i+1},\xi_i) + 2\alpha\bar{D}(\xi_i)\right\}\right]\Delta D(\xi_{t'/\delta t}) e^{-t'\hat{\mathcal{V}}} P(\xi_{t'/\delta t}) \\
&= \int d\xi \Delta D(\xi) e^{-(t-t')\hat{\mathcal{W}}} \Delta D(\xi) e^{-t'\hat{\mathcal{V}}} P(\xi).
\end{aligned}
\tag{B.1}
$$

Second, we derive Eq. (3.21). Eq. (3.7) also can be calculated as

$$
\begin{aligned}
\Omega(t,t',t'') &= \left\langle \Delta D(t)\Delta D(t') \exp\left[-2\alpha\int_{t''}^{t} d\tau \bar{D}(\tau) - 2\alpha\int_{t''}^{t'} d\tau' \bar{D}(\tau')\right] \bar{D}(t'') \right\rangle \\
&= \int \mathcal{D}\xi \Delta D(\xi(t)) \exp\left[-2\alpha\int_{t'}^{t} d\tau \bar{D}(\xi(\tau))\right] \Delta D(\xi(t')) \exp\left[-4\alpha\int_{t''}^{t'} d\tau' \bar{D}(\xi(\tau'))\right] \bar{D}(t'')\mathcal{P}[\xi] \\
&\approx \int \prod_{i=t''/\delta t}^{t/\delta t} d\xi_i \Delta D(\xi(t)) \exp\left[-2\alpha \sum_{i=t'/\delta t}^{t/\delta t-1} \delta t \bar{D}(\xi_i)\right] \Delta D(\xi_{t'/\delta t}) \exp\left[-4\alpha \sum_{i=t''/\delta t}^{t'/\delta t-1} \delta t \bar{D}(\xi_i)\right] \\
&\quad \times \exp\left[-\delta t \sum_{i=t''/\delta t}^{t/\delta t-1} s(\xi_{i+1},\xi_i)\right] \bar{D}(\xi_{t''/\delta t}) P(\xi_{t''/\delta t}) \\
&= \int \prod_{i=0}^{t/\delta t} d\xi_i \Delta D(\xi(t)) \exp\left[-\delta t \sum_{i=t'/\delta t}^{t/\delta t-1} \left\{s(\xi_{i+1},\xi_i) + 2\alpha\bar{D}(\xi_i)\right\}\right] \Delta D(\xi_{t'/\delta t}) \\
&\quad \times \exp\left[-\delta t \sum_{i=t''/\delta t}^{t'/\delta t-1} \left\{s(\xi_{i+1},\xi_i) + 4\alpha\bar{D}(\xi_i)\right\}\right] \bar{D}(\xi_{t''/\delta t}) P(\xi_{t''/\delta t}) \\
&= \int \prod_{i=t'/\delta t}^{t/\delta t} d\xi_i \Delta D(\xi(t)) \exp\left[-\delta t \sum_{i=t'/\delta t}^{t/\delta t-1} \left\{s(\xi_{i+1},\xi_i) + 2\alpha\bar{D}(\xi_i)\right\}\right] \Delta D(\xi_{t'/\delta t}) \\
&\quad \times e^{-(t'-t'')\hat{\mathcal{V}}} \bar{D}(\xi_{t'/\delta t}) P(\xi_{t'/\delta t}) \\
&= \int d\xi \Delta D(\xi) e^{-(t-t')\hat{\mathcal{W}}} \Delta D(\xi) e^{-(t'-t'')\hat{\mathcal{V}}} \bar{D}(\xi) P(\xi)
\end{aligned}
\tag{B.2}
$$

C Change of variables in FD dumbbell model

In this appendix we show the derivation of Eq. (3.25) by change the variables and perform the multiple integral.

First, we calculate the first term in the right hand side of Eq. (3.4). We apply change of variables as shown below.

$$x = \tau - \tau' \tag{C.1}$$
$$y = \tau' \tag{C.2}$$

Integral range of τ, τ' is

$$\tau' : 0 \to \tau \tag{C.3}$$
$$\tau : 0 \to t. \tag{C.4}$$

Therefore, from Fig. 2, the integral range of x, y is

$$x : 0 \to t \tag{C.5}$$
$$y : 0 \to t - x. \tag{C.6}$$

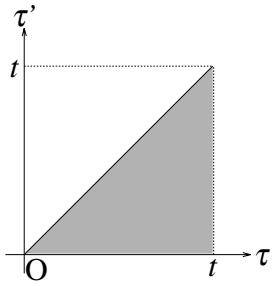

Figure 1: Integral range for τ, τ'

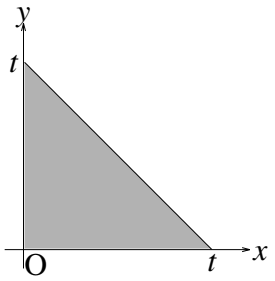

Figure 2: Integral range for x, y

The integral range is shown in Fig. 2.

Jacobian of this multiple integral is

$$J(x,y) = \frac{\partial(\tau',\tau)}{\partial(x,y)} = \begin{pmatrix} 0 & 1 \\ 1 & 1 \end{pmatrix}. \tag{C.7}$$

Also, from Eq. (3.19), Φ is depends only on $\tau - \tau' = x$. The first term of Eq. (3.4) can be calculated as

$$-n\alpha \int_0^t d\tau \int_0^\tau d\tau' \Phi(\tau,\tau') = -n\alpha \int_0^t dx \int_0^{t-x} dy |\det(J(x,y))| \Phi(x) = -n\alpha \int_0^t dx (t-x)\Phi(x). \tag{C.8}$$

With the same change of variables, the second term in the right hand side of Eq. (3.4) also can be rewritten as

$$\frac{n\alpha}{2} \int_0^t d\tau \int_0^\tau d\tau' \Psi(\tau,\tau') = \frac{n\alpha}{2} \int_0^t dx \int_0^{t-x} dy |\det(J(x,y))| \Psi(x,y) = \frac{n\alpha}{2} \int_0^t dx \int_0^{t-x} dy \Psi(x,y). \tag{C.9}$$

At last, we calculate third term in the right hand side of Eq. (3.4). To calculate this term, we use these change of variables as below.

$$x = \tau - \tau' \tag{C.10}$$
$$y = \tau' - \tau'' \tag{C.11}$$
$$z = \tau'' \tag{C.12}$$

Integral range of τ, τ', τ'' is

$$\tau'' : 0 \to \tau' \tag{C.13}$$
$$\tau' : 0 \to \tau \tag{C.14}$$
$$\tau : 0 \to t. \tag{C.15}$$
$$\tag{C.16}$$

The integral range is shown in Fig. 3. Therefore, we have the integral range of x, y, z as

$$x : 0 \to t \tag{C.17}$$
$$y : 0 \to t - x \tag{C.18}$$
$$z : 0 \to t - x - y, \tag{C.19}$$

which the range in shown in Fig. 4. Jacobian of the multiple integral is

$$J(x,y,z) = \frac{\partial(\tau,\tau',\tau'')}{x,y,z} = \begin{pmatrix} 1 & 1 & 1 \\ 0 & 1 & 1 \\ 0 & 0 & 1 \end{pmatrix}. \tag{C.20}$$

From, Eq. (3.21), Ω depends on only $\tau - \tau' = x, \tau' - \tau'' = y$. Therefore, the third term in the right hand side of Eq. (3.4) becomes

$$\begin{aligned} 2n\alpha^2 \int_0^t d\tau \int_0^\tau d\tau' \int_0^{\tau'} d\tau'' \Omega(\tau,\tau',\tau'') &= 2n\alpha^2 \int_0^t dx \int_0^{t-x} dy \int_0^{t-x-y} dz |\det(J(x,y,z))| \Omega(x,y) \\ &= 2n\alpha^2 \int_0^t dx \int_0^{t-x} dy (t-x-y)\Omega(x,y). \end{aligned} \tag{C.21}$$

Figure 3: Integral range for τ, τ', τ''

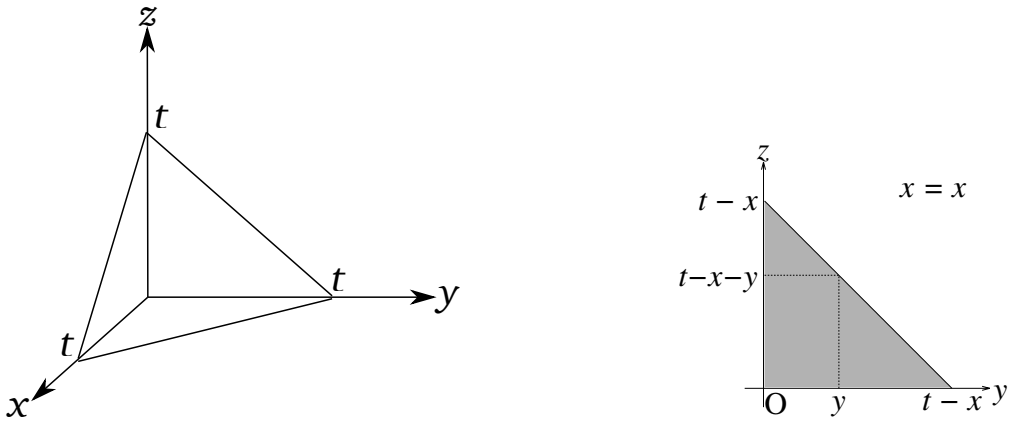

Figure 4: Integral range for x, y, z

D Calculation of expansion coefficients by engenmodes

In this appendix, we derive Eqs. (3.34) and (3.36) by using the eigenfunctions.

First, we show the derivation of the Eq. (3.34). We expand $\Delta D(\xi) P_{eq}(\xi)$ in Eq. (3.26) by using the basis set as

$$\Delta D(\xi) P_{eq}(\xi) = \sum_n c_n \psi_n(\xi). \tag{D.1}$$

By multiplying Eq. (D.1) by $\psi_m^\dagger(\xi)$ and integrate it about ξ, we obtain

$$\begin{aligned}\int d\xi \psi_m^\dagger(\xi)\Delta D(\xi)P_{eq}(\xi) &= \sum_n c_n \int d\xi \psi_m^\dagger(\xi)\psi_n(\xi) \\ &= \sum_n c_n \delta_{mn} \\ &= c_m,\end{aligned} \tag{D.2}$$

where c_m is expansion coefficient for $\Delta D(\xi)P_{eq}(\xi)$ in Eq. (3.26). Thus, we can obtain Eq. (3.34).

Second, we derive Eq. (3.36). $P_{eq}(\xi)$ can be expanded by eigenfunctions $\phi_m(\xi)$ as

$$P_{eq}(\xi) = \sum_m c_m^{(2)} \phi_m(\xi) \tag{D.3}$$

$$c_m^{(2)} = \int d\xi' \phi_m^\dagger(\xi') P_{eq}(\xi'). \tag{D.4}$$

Expansion coefficient $c_m^{(2)}$ can be obtained in the same way as Eq. (D.2). Therefore, Eq. (3.27) can be rewritten as

$$\begin{aligned}\Psi(t,s) &= \int d\xi \Delta D(\xi) e^{-t\hat{\mathcal{W}}} \Delta D(\xi) e^{-s\hat{\mathcal{V}}} \sum_m c_m^{(2)} \phi_m(\xi) \\ &= \int d\xi \Delta D(\xi) e^{-t\hat{\mathcal{W}}} \Delta D(\xi) \sum_m c_m^{(2)} e^{-\mu_m s} \phi_m(\xi) \\ &= \sum_m c_m^{(2)} e^{-\mu_m s} \int d\xi \Delta D(\xi) e^{-t\hat{\mathcal{W}}} \Delta D(\xi) \phi_m(\xi).\end{aligned} \tag{D.5}$$

Also, $\Delta D(\xi)\phi_m(\xi)$ can be expanded by eigenfunctions $\psi_n(\xi)$ as shown below.

$$\Delta D(\xi)\phi_m(\xi) = \sum_n c_{mn}^{(3)} \psi_n(\xi) \tag{D.6}$$

$$c_{mn}^{(3)} = \int d\xi'' \psi_n^\dagger(\xi'') \Delta D(\xi'') \phi_m(\xi''). \tag{D.7}$$

Therefore, Eq. (D.5) can be calculated as

$$\begin{aligned}\Psi(t,s) &= \sum_m c_m^{(2)} e^{-\mu_m s} \int d\xi \Delta D(\xi) e^{-t\hat{\mathcal{W}}} \sum_n c_{mn}^{(3)} \psi_n(\xi) \\ &= \sum_m c_m^{(2)} e^{-\mu_m s} \int d\xi \Delta D(\xi) \sum_n c_{mn}^{(3)} e^{-t\lambda_n} \psi_n(\xi) \\ &= \sum_n \sum_m c_m^{(2)} c_{mn}^{(3)} e^{-\mu_m s} e^{-t\lambda_n} \int d\xi \Delta D(\xi) \psi_n(\xi),\end{aligned} \tag{D.8}$$

and we have Eq. (3.36).

E Derivation of correlation function in TS dumbbell model

In this appendix, we show the derivation of Eq. (3.50). From, Eq. (3.26), we have

$$\Phi(t) = (1\ 1\ 1\ 1)\Delta\mathcal{D}\ e^{-t\mathcal{W}} \Delta\mathcal{D}\boldsymbol{P}_{eq}. \tag{E.1}$$

Due to the nature of diagonalization,

$$\boldsymbol{\psi}^{-1}\mathcal{W}\boldsymbol{\psi} = \Lambda \tag{E.2}$$

$$\therefore\ \boldsymbol{\psi}^{-1}\mathcal{W}^k\boldsymbol{\psi} = \Lambda^k. \tag{E.3}$$

Besides, the matrix exponential function is defined as

$$e^A = E + A + \frac{A^2}{2!} + \frac{A^3}{3!} + \cdots . \tag{E.4}$$

Therefore, $e^{-t\mathcal{W}}$ can be calculated as

$$\begin{aligned} e^{-t\mathcal{W}} &= E + (-t\mathcal{W}) + \frac{(-t\mathcal{W})^2}{2!} + \frac{(-t\mathcal{W})^3}{3!} + \cdots \\ &= \boldsymbol{\psi}\left(E + (-t\Lambda) + \frac{(-t\Lambda)^2}{2!} + \frac{(-t\Lambda)^3}{3!} + \cdots\right)\boldsymbol{\psi}^{-1} \\ &= \boldsymbol{\psi}e^{-t\Lambda}\boldsymbol{\psi}^{-1}. \end{aligned} \tag{E.5}$$

Then, we have Eq. (3.50).

F Derivation of transition matrix in TS model

In this appendix, we derive the transition matrix in TS dumbbell model.

At first, we derive the transition possibilities by solving Eq. (3.49). The formal solution of Eq. (3.49) is

$$\begin{pmatrix} P_f(t+\delta t) \\ P_s(t+\delta t) \end{pmatrix} = \exp\left[-\delta t \begin{pmatrix} -k_f & k_s \\ k_f & -k_s \end{pmatrix}\right] \begin{pmatrix} P_f(t) \\ P_s(t) \end{pmatrix}. \tag{F.1}$$

By diagonalizing the transition matrix in Eq. (3.49), we have

$$\begin{aligned} \begin{pmatrix} P_f(t+\delta t) \\ P_s(t+\delta t) \end{pmatrix} &= \exp\left[-\delta t \begin{pmatrix} k_s & 1 \\ k_f & -1 \end{pmatrix}\begin{pmatrix} -k_f & k_s \\ k_f & -k_s \end{pmatrix}\begin{pmatrix} k_s & 1 \\ k_f & -1 \end{pmatrix}^{-1}\right] \begin{pmatrix} P_f(t) \\ P_s(t) \end{pmatrix} \\ &= \frac{1}{k_f + k_s}\begin{pmatrix} k_s + k_f e^{-\delta t(k_f+k_s)} & k_s\left(1 - e^{-\delta t(k_f+k_s)}\right) \\ k_f\left(1 - e^{-\delta t(k_f+k_s)}\right) & k_f + k_s e^{-\delta t(k_f+k_s)} \end{pmatrix}. \end{aligned} \tag{F.2}$$

Therefore, the transition possibilities for $f \to s$ and $s \to f$ in δt are derived as

$$w_{fs} = \frac{k_f}{k_f + k_s}\left(1 - e^{-\delta t(k_f+k_s)}\right), \tag{F.3}$$

$$w_{sf} = \frac{k_s}{k_f + k_s}\left(1 - e^{-\delta t(k_f+k_s)}\right), \tag{F.4}$$

respectively. Using this result, we can obtain the time evolution of the state possibilities of the

dumbbell as

$$\boldsymbol{P}_{eq}(t+\delta t) = \begin{pmatrix} P(ff, t+\delta t) \\ P(fs, t+\delta t) \\ P(sf, t+\delta t) \\ P(ss, t+\delta t) \end{pmatrix}$$
$$= \begin{pmatrix} (1-w_{fs})(1-w_{fs}) & (1-w_{fs})w_{sf} & w_{sf}(1-w_{fs}) & w_{sf}w_{sf} \\ (1-w_{fs})w_{fs} & (1-w_{fs})(1-w_{sf}) & w_{sf}w_{fs} & w_{sf}(1-w_{sf}) \\ w_{fs}(1-w_{fs}) & w_{fs}w_{sf} & (1-w_{sf})(1-w_{fs}) & (1-w_{sf})w_{sf} \\ w_{fs}w_{fs} & w_{fs}(1-w_{sf}) & (1-w_{sf})w_{fs} & (1-w_{sf})(1-w_{sf}) \end{pmatrix} \begin{pmatrix} P(ff, t) \\ P(fs, t) \\ P(sf, t) \\ P(ss, t) \end{pmatrix}$$
$$\equiv \mathcal{M}\boldsymbol{P}_{eq}(t). \tag{F.5}$$

At the limit of $\delta t \to 0$, we have

$$\boldsymbol{P} + \delta t \frac{d}{dt}\boldsymbol{P}(t) = \mathcal{M}\boldsymbol{P}(t) \tag{F.6}$$
$$\therefore \ \frac{d}{dt}\boldsymbol{P}(t) = \frac{1}{\delta t}\left(\mathcal{M} - I\right)\boldsymbol{P}(t) = \mathcal{L}\boldsymbol{P}(t) \tag{F.7}$$
$$\mathcal{L} = \frac{1}{\delta t}\left(\mathcal{M} - I\right) \to \begin{pmatrix} -2k_f & k_s & k_s & 0 \\ k_f & -k_f - k_s & 0 & k_s \\ k_f & 0 & -k_f - k_s & k_s \\ 0 & k_f & k_f & -2k_f \end{pmatrix}, \tag{F.8}$$

where I is a unit matrix with the size of 4×4. Then, we can derive Eq. (3.62).

Bibliography

[1] Robert Byron Bird, Charles F. Curtiss, Robert C. Armstrong, and Ole Hassager. *Dynamics of Polymeric Liquids, Volume 2: Kinetic Theory, 2nd Edition*. Wiley, 2nd edition, 1987.

[2] M. Doi, S.F. Edwards, and S.F. Edwards. *The Theory of Polymer Dynamics*. Comparative Pathobiology - Studies in the Postmodern Theory of Education. Clarendon Press, 1988.

[3] Prince E. Rouse. A theory of the linear viscoelastic properties of dilute solutions of coiling polymers. *The Journal of Chemical Physics*, 21(7):1272–1280, 1953.

[4] Harold R. Warner. Kinetic Theory and Rheology of Dilute Suspensions of Finitely Extendible Dumbbells. *Industrial and Engineering Chemistry Fundamentals*, 11(3):379–387, 1972.

[5] Xi Jun Fan. Viscosity, first normal-stress coefficient, and molecular stretching in dilute polymer solutions. *Journal of Non-Newtonian Fluid Mechanics*, 17(2):125–144, 1985.

[6] John G. Kirkwood and Jacob Riseman. The intrinsic viscosities and diffusion constants of flexible macromolecules in solution. *The Journal of Chemical Physics*, 16(6):565–573, 1948.

[7] H. Giesekus. A simple constitutive equation for polymer fluids based on the concept of deformation-dependent tensorial mobility. *Journal of Non-Newtonian Fluid Mechanics*, 11(1-2):69–109, 1982.

[8] Elliott W. Montroll and George H. Weiss. Random Walks on Lattices. II. *Journal of Mathematical Physics*, 6(167), 1965.

[9] Jean-Philippe Bouchaud. Weak ergodicity breaking and aging in disordered systems. *Journal de Physique I*, 2(9):1705–1713, 1992.

[10] Felix Höfling and Thomas Franosch. Anomalous transport in the crowded world of biological cells. *Reports on Progress in Physics*, 76(4), 2013.

[11] Vincent Tejedor, Olivier Bénichou, Raphael Voituriez, Ralf Jungmann, Friedrich Simmel, Christine Selhuber-Unkel, Lene B. Oddershede, and Ralf Metzler. Quantitative analysis of single particle trajectories: Mean maximal excursion method. *Biophysical Journal*, 98(7):1364–1372, 2010.

[12] Jae Hyung Jeon, Vincent Tejedor, Stas Burov, Eli Barkai, Christine Selhuber-Unkel, Kirstine Berg-Sørensen, Lene Oddershede, and Ralf Metzler. In vivo anomalous diffusion and weak ergodicity breaking of lipid granules. *Physical Review Letters*, 106(4):2–5, 2011.

[13] Ronald Forrest Fox. The generalized Langevin equation with Gaussian fluctuations. *Journal of Mathematical Physics*, 18(12):2331–2335, 1976.

[14] K. Kawasaki. Simple derivations of generalized linear and nonlinear Langevin equations. *Journal of Physics A: General Physics*, 6(9):1289–1295, 1973.

[15] T. G. Mason and D. A. Weitz. Optical measurements of frequency-dependent linear viscoelastic moduli of complex fluids. *Physical Review Letters*, 74(7):1250–1253, 1995.

[16] Joel D. Eaves and David R. Reichman. Spatial dimension and the dynamics of supercooled liquids. *Proceedings of the National Academy of Sciences of the United States of America*, 106(36):15171–15175, 2009.

[17] Bo Wang, Stephen M. Anthony, Chul Bae Sung, and Steve Granick. Anomalous yet Brownian. *Proceedings of the National Academy of Sciences of the United States of America*, 106(36):15160–15164, 2009.

[18] Toshihiro Toyota, David A. Head, Christoph F. Schmidt, and Daisuke Mizuno. Non-Gaussian athermal fluctuations in active gels. *Soft Matter*, 7(7):3234–3239, 2011.

[19] Tomoshige Miyaguchi, Takuma Akimoto, and Eiji Yamamoto. Langevin equation with fluctuating diffusivity: A two-state model. *Physical Review E*, 94(1):1–21, 2016.

[20] Aleksei V. Chechkin, Flavio Seno, Ralf Metzler, and Igor M. Sokolov. Brownian yet non-Gaussian diffusion: From superstatistics to subordination of diffusing diffusivities. *Physical Review X*, 7(2):1–20, 2017.

[21] Vittoria Sposini, Aleksei V. Chechkin, Flavio Seno, Gianni Pagnini, and Ralf Metzler. Random diffusivity from stochastic equations: Comparison of two models for Brownian yet non-Gaussian diffusion. *New Journal of Physics*, 20(4), 2018.

[22] Takashi Uneyama, Tomoshige Miyaguchi, and Takuma Akimoto. Relaxation functions of the Ornstein-Uhlenbeck process with fluctuating diffusivity. *Physical Review E*, 99(3):1–13, 2019.

[23] Hans Sillescu. Heterogeneity at the glass transition: A review. *Journal of Non-Crystalline Solids*, 243(2-3):81–108, 1999.

[24] Mykyta V. Chubynsky and Gary W. Slater. Diffusing diffusivity: A model for anomalous, yet Brownian, diffusion. *Physical Review Letters*, 113(9):1–5, 2014.

[25] Takashi Uneyama, Tomoshige Miyaguchi, and Takuma Akimoto. Fluctuation analysis of time-averaged mean-square displacement for the Langevin equation with time-dependent and fluctuating diffusivity. *Physical Review E - Statistical, Nonlinear, and Soft Matter Physics*, 92(3):1–17, 2015.

[26] Nabi Ahamad and Pallavi Debnath. Rouse model in crowded environment modeled by " diffusing diffusivity ". *Physica A: Statistical Mechanics and its Applications*, 549:124335, 2020.

[27] D J Evans and Morris G P. *Statistical Mechanics of Nonequilibrium Liquids*. Cambridge. Cambridge University Press, 2nd edition, 2008.

[28] Rebecca L. Honeycutt. Stochastic Runge-Kutta algorithms. I. White noise Rebecca. *Physical Review A*, 45(2):5, 2011.

[29] C. Bennemann, J. Baschnagel, W. Paul, and K. Binder. Molecular-dynamics simulation of a glassy polymer melt: Rouse model and cage effect. *Computational and Theoretical Polymer Science*, 9(3-4):217–226, 1999.

[30] Tomoshige Miyaguchi, Takashi Uneyama, and Takuma Akimoto. Brownian motion with alternately fluctuating diffusivity: Stretched-exponential and power-law relaxation. *Physical Review E*, 100(1):19–24, 2019.

[31] Takashi Uneyama, Takuma Akimoto, and Tomoshige Miyaguchi. Crossover time in relative fluctuations characterizes the longest relaxation time of entangled polymers. *Journal of Chemical Physics*, 137(11), 2012.

[32] Alexei E. Likhtman. Single-chain slip-link model of entangled polymers: Simultaneous description of neutron spin-echo, rheology, and diffusion. *Macromolecules*, 38(14):6128–6139, 2005.